Robotica (2022), **40**, pp. 997–1019
doi:10.1017/S0263574721000977

CAMBRIDGE
UNIVERSITY PRESS

RESEARCH ARTICLE

Robust fuzzy sliding mode control and vibration suppression of free-floating flexible-link and flexible-joints space manipulator with external interference and uncertain parameter

Limin Xie[1,*], Xiaoyan Yu[2], and Li Chen[2]

[1]College of Mechanical and Electrical Engineering, Fujian Agriculture and Forestry University, Fuzhou 350003, Fujian, China and [2]School of Mechanical Engineering and Automation, Fuzhou University, Fuzhou 350016, Fujian, China
*Corresponding author. E-mail: lucy_min@163.com

Received: 15 October 2020; **Revised:** 6 May 2021; **Accepted:** 24 June 2021; **First published online:** 2 August 2021

Keywords: free-floating flexible-link and flexible-joints space manipulator; singular perturbation; robust; fuzzy; vibration suppression

Abstract
The flexibility of the free-floating flexible space manipulator system's link and joint may affect the control accuracy and cause vibrations. We studied the dynamics modeling, joint trajectory tracking control, and vibration suppressing problem of free-floating flexible-link and flexible-joints space manipulator system with external interference and uncertain parameter. The system's dynamic equations are established using linear momentum conservation, angular momentum conservation, assumed mode method, and Lagrange equation. Then, the system's singular perturbation model is established, and a hybrid control is presented. For the slow subsystem, a robust fuzzy sliding mode control is proposed to realize the joint desired trajectory tracking. For the fast subsystem, a speed difference feedback control and a linear-quadratic optimal control are designed to suppress the vibration caused by the flexible joints and the flexible link separately. The simulation comparison experiments under different conditions are taken. The simulate results demonstrate the proposed hybrid control's validity.

1. Introduction

With the development of space technology, especially the successful application of the space station, space shuttles, space robot, etc., the space manipulator, as a critical technology of in-orbit support and service, has shown strong application ability and broad application prospect and has played a significant, influential role in the development of space science and application. There are considerable achievements in the research of the space manipulator [1, 2, 3, 4, 5, 6, 7, 8, 9, 10, 11, 12]. Many control methods have been proposed, such as PID control, robust control [13, 14, 15], adaptive control [16, 17, 18], fuzzy control, neural network control, and many hybrid control methods [19, 20, 21, 22, 23, 24, 25, 26].

Most of the current researches usually assume that space manipulator is a rigid system. But, in practice, the space manipulator often contains flexible components, such as the flexible joint and the flexible link. The flexible link has lightweight, less inertia, low energy consumption, sizeable working place, and high work efficiency. But, it may deform and vibrate [27, 28, 29]. The flexible joint, caused by the harmonic drive gears, can reduce the damage caused by a collision when the manipulator grabs the target object and can compensate for the torque. But, it will cause error and vibration [30, 31, 32].

With the increasing requirement of lightweight, high speed, and high precision, we cannot ignore the influence of flexibility. Especially for the free-floating flexible space manipulator system, the system is nonlinear and strongly coupled. The flexible link makes the system uncertain; the flexible joints make the system's degrees of freedom be twice the number of control inputs. So, the dynamic analysis and the motion control design become difficult. There are some researches on the flexible space manipulator, and many control methods are proposed. Komats [33] had dynamical analysis for a redundant flexible space manipulator with slewing and deployable links on the space platform. Wu [34] proposed an optimal trajectory planning method with vibration reduction for a dual-arm space robot with flexible links using Particle Swarm Optimization (PSO). Xie [35] offered a robust and adaptive control for the free-floating flexible space manipulator with bounded control torques. Sabatini [36] presented an optimized adaptive vibration control via piezoelectric devices for a space manipulator with flexible links during its on-orbit operations. Huang [37] carried out some simulation experiments on the trajectory tracking of multi-flexible-link space robot with a dead zone. Kumar [38] developed a simplified model controller that only needs the space robot's base velocity and link parameters. Kayastha [39] adopted linear quadratic regulator (LQR) and model predictive control (MPC) algorithms to control the motion of a two-link flexible space robot system under external force. But, they are only for the space manipulator with flexible link. Yu [40] proposed an observer-based two-time scale robust control of free-flying flexible-joint space manipulators. Nanos [41] established the flexible-joint space manipulator dynamics model. Ulrich proposed an adaptive trajectory control [42], an extended Kalman filter (EKF) strategy [43], and a nonlinear adaptive output feedback control [44] for the flexible-joint space manipulator. Liang [45] discussed a radial basis function neural network adaptive control and elastic vibration suppression for flexible-joint space robots with unknown parameters. But, they are only for the space manipulator with flexible joint. The researches on the space manipulator with both flexible link and flexible joint are few. Dong [46] considered the flexibility of joint and link and discussed the dynamic modeling and analysis of space manipulator. Xie [47] established the free-floating flexible-joint and flexible-link space robot's singular perturbation model and proposed a nonlinear sliding mode motion control. Zhang [48] designed a trajectory tracking controller with friction compensation based on the computed torque method. Yu [49] offered an augmented robust control method based on a singularly perturbed model. Zhang [50] designed a L_2 -gain robust control for space robot with flexible joints and flexible link, which directly avoided solving the HJI inequality.

Simultaneously, we notice that some physical parameters of the space manipulator system are uncertain or time varying due to the changes in parameters, load, fuel, etc. [51,52] So, the controller, which is usually used for the fixed base manipulator, is challenging to apply to the space manipulator's control directly. Meanwhile, the space manipulator system will inevitably be affected by the friction between the arm joints, movement noise, fuel change, solar wind, particle ray flow, and other external interference.

To save fuel, prolong the space robot system's service life, and reduce the launch cost, it is essential to study the free-floating space manipulator in which the base's position and attitude are not actively controlled [53]. In this paper, the dynamic modeling, motion control, and double vibration active suppression for the free-floating flexible-link and flexible-joint space manipulator system with external interference and uncertain parameters are studied. We consider the flexibility of the link and joints. The system's dynamic equations are established according to linear momentum conservation, angular momentum conservation, assumed mode method [54], and Lagrange equation. To facilitate the design of the control, according to the singular perturbation theory [55], the system is decomposed into three subsystems:

- the slow subsystem
- the flexible-joints fast subsystem
- the flexible-link fast subsystem

Then, for the slow subsystem, a robust fuzzy sliding mode control is proposed. It can compensate for the system's uncertain parameters and external interference by the robust controller and can reduce the chattering of sliding mode control by the saturated function and the fuzzy controller. And, the fuzzy controller is designed based on the results of the system stability analysis. For the flexible-joints fast subsystem, a velocity difference feedback controller is designed to suppress the flexible-joints vibration. For the flexible-link fast subsystem, a linear quadratic regulator (LQR) [56] is presented to stop the flexible-link vibration. Finally, the MATLAB simulations with different desired trajectories and external

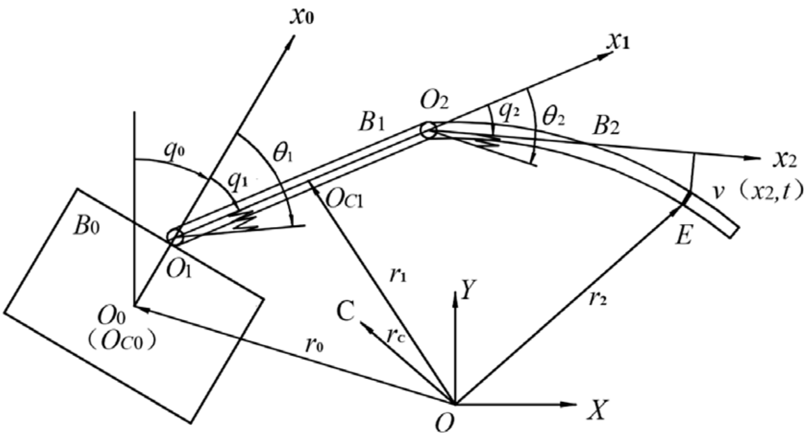

Figure 1. *Free-floating flexible-link and flexible-joints space manipulator.*

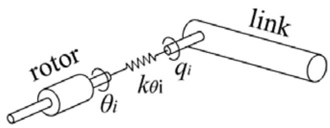

Figure 2. *The simple model of flexible joint.*

interference are taken to verify the proposed controller's effectiveness. The simulation results proved that the proposed hybrid control could control the system to track the desired trajectory accurately and suppress the vibration caused by the flexible joints and the flexible link.

The main contributions of this study are summarized as follows:

(1) Both flexible link and flexible joint are considered in the space manipulator system.

(2) The uncertain parameters and external interference are considered.

(3) The dynamic model of the system is established and decomposed by the singular perturbed method.

(4) A hybrid controller is proposed to track the desired trajectory and suppress the vibration caused by the flexible joints and the flexible link.

2. System dynamic analysis and modeling

The free-floating flexible-link and flexible-joints space manipulator system is composed of a rigid base B_0, a rigid link B_1, a flexible link B_2, and two flexible joints $O_i(i = 1, 2)$, as shown in Fig. 1. $\boldsymbol{OXY}$ is the inertial coordinate system, and $O_jx_jy_j$ is the main axis coordinate of B_j ($j = 0, 1, 2$). The centroids of B_0, B_1, and the system are O_{c0}, O_{c1}, and C. Their position vectors are $\boldsymbol{r}_0$, $\boldsymbol{r}_1$, and $\boldsymbol{r}_c$. The arbitrary point's position vector on the flexible link B_2 is r_2. q_j is the motion angle of B_j. θ_i is the motor rotor's angle.

According to Spong's assumption [57], we regard the flexible joints O_i as a linear spring between the motor rotor and the link and the spring's stiffness coefficient is $k_{\theta i}$, as shown in Fig. 2. In this case, the rotor's rotation angle θ_i will not always equal the link's rotation angle q_i. And, the flexible-joint error is: $\sigma_i = \theta_i - q_i$.

The flexible link B_2 is considered as an Euler–Bernoulli beam [58]. Neglecting the rotational inertia and shear deformation, based on the assumed mode method, the flexible link's elastic deformation is:

$$\upsilon(x_2, t) = \sum_{i=1}^{n} \varphi_i(x_2)\delta_i(t) \tag{1}$$

https://doi.org/10.1017/S0263574721000977 Published online by Cambridge University Press

where $\varphi t_i(x_2)$ is the i th mode function, $\delta_i(t)$ is the i th mode coordinate, and n is the retention mode number. Considering that the lower order modes play a leading role in elastic vibration and deformation, the first two lower-order modes can meet the accuracy requirements and reduce the calculation [59,60]. So, we choose $n = 2$, that is, $\upsilon(x_2, t) = \varphi_1(x_2)\delta_1(t) + \varphi_2(x_2)\delta_2(t)$.

According to the geometric position relationship

$$\begin{cases} \boldsymbol{r}_1 = \boldsymbol{r}_0 + l_0\boldsymbol{e}_0 + d_1\boldsymbol{e}_1 \\ \boldsymbol{r}_2 = \boldsymbol{r}_0 + l_0\boldsymbol{e}_0 + l_1\boldsymbol{e}_1 + x_2\boldsymbol{e}_2 + \upsilon(x_2, t)\boldsymbol{e}_3 \end{cases} \tag{2}$$

where l_0 is the distance between O_{c0} and O_1, d_1 is the distance between O_1 and O_{c1}, l_1 is the length of B_1.

$$e_0 = \begin{bmatrix} \sin(q_0) \\ \cos(q_0) \end{bmatrix}^{\mathrm{T}}, e_1 = \begin{bmatrix} \sin(q_0 + q_1) \\ \cos(q_0 + q_1) \end{bmatrix}^{\mathrm{T}}, e_2 = \begin{bmatrix} \sin(q_0 + q_1 + q_2) \\ \cos(q_0 + q_1 + q_2) \end{bmatrix}^{\mathrm{T}}, e_3 = \begin{bmatrix} \cos(q_0 + q_1 + q_2) \\ -\sin(q_0 + q_1 + q_2) \end{bmatrix}^{\mathrm{T}}.$$

The system's total center theorem of mass is:

$$m_0\boldsymbol{r}_0 + m_1\boldsymbol{r}_1 + \rho\int_0^{l_2} \boldsymbol{r}_2 \mathrm{d}x_2 = M\boldsymbol{r}_c \tag{3}$$

where m_0 is the mass of B_0, m_1 is the mass of B_1, ρ is the linear density of B_2, and l_2 is the length of B_2. M is the total system's mass, $M = m_0 + m_1 + \rho l_2$. The mass of the motor is negligible.

The position vectors can be expressed as follows:

$$\boldsymbol{r}_i = \boldsymbol{r}_c + R_{i0}\boldsymbol{e}_0 + R_{i1}\boldsymbol{e}_1 + R_{i2}\boldsymbol{e}_2 + (R_{i3}\delta_1 + R_{i4}\delta_2)\boldsymbol{e}_3 \tag{4}$$

where $R_{00} = -(m_1 + \rho l_2)l_0/M, R_{01} = -(m_1 d_1 + \rho l_2 l_1)/M, R_{02} = -\rho l_2^2/(2M), R_{03} = -\rho\int_0^{l_2}\varphi_1(x_2)dx_2/M$, $R_{04} = -\rho\int_0^{l_2}\varphi_2(x_2)dx_2/M, R_{10} = R_{00} + l_0, R_{11} = R_{01} + d_1, R_{12} = R_{02}, R_{13} = R_{03}, R_{14} = R_{04}, R_{20} = R_{00} + l_0$, $R_{21} = R_{01} + l_1$, $R_{22} = R_{02} + x_2$, $R_{23} = R_{03} + \varphi_1(x_2)$, $R_{24} = R_{04} + \varphi_2(x_2)$.

Differentiating Eq. (4), we have:

$$\dot{\boldsymbol{r}}_i = \dot{\boldsymbol{r}}_c + R_{i0}\dot{\boldsymbol{e}}_0 + R_{i1}\dot{\boldsymbol{e}}_1 + R_{i2}\dot{e}_2 + (R_{i3}\delta_1 + R_{i4}\delta_2)\dot{\boldsymbol{e}}_3 + (R_{i3}\dot{\delta}_1 + R_{i4}\dot{\delta}_2)\boldsymbol{e}_3 \tag{5}$$

where $\dot{\boldsymbol{r}}_i$, $\dot{\boldsymbol{r}}_c$, $\dot{\delta}_1$, and $\dot{\delta}_2$ are the first derivative of $\boldsymbol{r}_i$, $\boldsymbol{r}_c$, δ_1, and δ_2. $\dot{\boldsymbol{e}}_0 = \dot{q}_0\begin{bmatrix} \cos(q_0) \\ -\sin(q_0) \end{bmatrix}^{\mathrm{T}}$, $\dot{\boldsymbol{e}}_1 = (\dot{q}_0 + \dot{q}_1)\begin{bmatrix} \cos(q_0 + q_1) \\ -\sin(q_0 + q_1) \end{bmatrix}^{\mathrm{T}}$, $\dot{\boldsymbol{e}}_2 = (\dot{q}_0 + \dot{q}_1 + \dot{q}_2)\begin{bmatrix} \cos(q_0 + q_1 + q_2) \\ -\sin(q_0 + q_1 + q_2) \end{bmatrix}^{\mathrm{T}}$, and $\dot{\boldsymbol{e}}_3 = (\dot{q}_0 + \dot{q}_1 + \dot{q}_2)\begin{bmatrix} -\sin(q_0 + q_1 + q_2) \\ -\cos(q_0 + q_1 + q_2) \end{bmatrix}^{\mathrm{T}}$.

Without loss of generality, the system satisfies the momentum conservation and the angular momentum conservation. Let the initial values of the momentum and the angular momentum be zero, the system's momentum conservation equation and the angular momentum conservation equation can be expressed as:

$$m_0\dot{\boldsymbol{r}}_0 + m_1\dot{\boldsymbol{r}}_1 + \rho\int_0^{l_2} \dot{\boldsymbol{r}}_2 \mathrm{d}x_2 = 0 \tag{6}$$

$$(m_0\boldsymbol{r}_0 \times \dot{\boldsymbol{r}}_0 + J_0\omega_0) + (m_1\boldsymbol{r}_1 \times \dot{\boldsymbol{r}}_1 + J_1\omega_1) + \rho\int_0^{l_2} (\boldsymbol{r}_2 \times \dot{\boldsymbol{r}}_2)\mathrm{d}x_2 + \sum_{i=1}^{2}(J_{\theta i}\omega_{\theta i}) = 0 \tag{7}$$

where J_0 is the inertial moment of B_0, J_1 is the inertial moment of B_1, and $J_{\theta i}$ is the inertial moment of the motor rotor. ω_0 is the angular velocity of B_0, $\omega_0 = \dot{q}_0$. ω_1 is the angular velocity of B_1, $\omega_1 = (\dot{q}_0 + \dot{q}_1)$. $\omega_{\theta i}$ is the angular velocity of motor rotor, $\omega_{\theta i} = \dot{\theta}_i$.

https://doi.org/10.1017/S0263574721000977 Published online by Cambridge University Press

The system's kinetic energy T contains the manipulator system's kinetic energy T_r and the motor rotors' kinetic energy T_θ:

$$T = T_r + T_\theta \tag{8}$$

where $T_r = T_0 + T_1 + T_2$, $T_\theta = T_{\theta 1} + T_{\theta 2}$. $T_0 = \frac{1}{2}m_0\dot{\boldsymbol{r}}_0^2 + \frac{1}{2}J_0\omega_0^2$ is B_0 's kinetic energy, $T_1 = \frac{1}{2}m_1\dot{\boldsymbol{r}}_1^2 + \frac{1}{2}J_1\omega_1^2$ is B_1 's kinetic energy, $T_2 = \frac{1}{2}\rho\int_0^{l_2}\dot{\boldsymbol{r}}_2^2\mathrm{d}\boldsymbol{x}_2$ is B_2 's kinetic energy, $T_{\theta i} = \frac{1}{2}J_{\theta i}\omega_{\theta i}^2$ is the motor rotor's kinetic energy.

Neglecting the gravity in the space. The system's potential energy U contains the flexible link's bending strain energy U_r and the flexible joints' elastic deformation potential energy U_θ:

$$U = U_r + U_\theta \tag{9}$$

where $U_r = \frac{1}{2}EI\int_0^{l_2}\left(\frac{\partial^2 v(x_2,t)}{\partial x_2^2}\right)^2\mathrm{d}x_2$, $U_\theta = \frac{1}{2}\sum_{i=1}^{2}k_{\theta i}(\theta_i - q_i)^2$, EI is the bending stiffness of B_2.

The system's Lagrangian function is: $L = T - U$. Choose $\boldsymbol{Q} = \begin{bmatrix}\theta_1 & \theta_2 & q_0 & q_1 & q_2 & \delta_1 & \delta_2\end{bmatrix}^{\mathrm{T}}$ as the system's generalized coordinate, $\boldsymbol{F} = \begin{bmatrix}\tau_1 & \tau_2 & 0 & 0 & 0 & 0 & 0\end{bmatrix}^{\mathrm{T}}$ as the generalized force. Then, according to Lagrange's second type equation $\frac{\mathrm{d}}{\mathrm{d}t}\left(\frac{\partial L}{\partial \dot{\boldsymbol{Q}}}\right) - \frac{\partial L}{\partial \boldsymbol{Q}} = \boldsymbol{F}$, the system's dynamic equation has the following form

$$\boldsymbol{J}_\theta\ddot{\boldsymbol{\theta}} + \boldsymbol{K}_\theta(\boldsymbol{\theta} - \boldsymbol{q}_\theta) = \boldsymbol{\tau} + \boldsymbol{\tau}_{\mathrm{d}} \tag{10a}$$

$$\boldsymbol{M}(\boldsymbol{q},\boldsymbol{\delta})\begin{bmatrix}\ddot{\boldsymbol{q}}\\ \ddot{\boldsymbol{\delta}}\end{bmatrix} + \boldsymbol{H}(\boldsymbol{q},\dot{\boldsymbol{q}},\boldsymbol{\delta},\dot{\boldsymbol{\delta}})\begin{bmatrix}\dot{\boldsymbol{q}}\\ \dot{\boldsymbol{\delta}}\end{bmatrix} + \begin{bmatrix}0\\ -\boldsymbol{K}_\theta(\boldsymbol{\theta} - \boldsymbol{q}_\theta)\\ \boldsymbol{K}_\delta\boldsymbol{\delta}\end{bmatrix} = 0 \tag{10b}$$

where $\boldsymbol{\theta} = [\theta_1 \quad \theta_2]^{\mathrm{T}}$, $\boldsymbol{q}_\theta = [q_1 \quad q_2]^{\mathrm{T}}$, $\boldsymbol{q} = [q_0 \quad q_1 \quad q_2]^{\mathrm{T}}$, $\boldsymbol{\delta} = [\delta_1 \quad \delta_2]^{\mathrm{T}}$, $\boldsymbol{J}_\theta = \mathrm{diag}(J_{\theta 1}, J_{\theta 2}) \in \boldsymbol{R}^{2\times 2}$ is the diagonal and positive definite inertia matrix of the motor, $\boldsymbol{K}_\theta = \mathrm{diag}(k_{\theta 1}, k_{\theta 2}) \in \boldsymbol{R}^{2\times 2}$ is the simplified linear spring stiffness coefficient matrix of flexible joint, $\boldsymbol{M}(\boldsymbol{q},\boldsymbol{\delta}) \in \boldsymbol{R}^{5\times 5}$ is the space manipulator's symmetric positive definite inertia matrix, $\boldsymbol{H}(\boldsymbol{q},\dot{\boldsymbol{q}},\boldsymbol{\delta},\dot{\boldsymbol{\delta}})\begin{bmatrix}\dot{\boldsymbol{q}}\\ \dot{\boldsymbol{\delta}}\end{bmatrix} \in \boldsymbol{R}^{5\times 1}$ is a column vector containing the Coriolis force and centrifugal force, $\boldsymbol{K}_\delta = \mathrm{diag}(k_{\delta 1}, k_{\delta 2})$ is the flexible link's stiffness coefficient matrix, $k_{\delta i} = \int_0^{l_2} EI\varphi_i''^{\mathrm{T}}\varphi_i''\mathrm{d}x_2$. $\boldsymbol{\tau} = [\tau_1 \quad \tau_2]^{\mathrm{T}} \in \boldsymbol{R}^{2\times 1}$ is the output torque of the motors, and $\boldsymbol{\tau}_{\mathrm{d}} \in \boldsymbol{R}^{2\times 1}$ is the external interference torque.

It can be seen that Eq. (10a) is the dynamic equation of the motor and Eq. (10b) is the dynamic equation of the space manipulator.

3. Singular perturbation decomposition and control design

The free-floating flexible-link and flexible-joints space manipulator system is a rigid-flexible coupling system. The interaction between the rigid variables and the flexible variables will make the controller's design difficult and affect the control quality. To reduce the interaction between variables, we use the singular perturbation method to decompose the complex system into a slow subsystem and a fast subsystem with independent time scales. The slow subsystem describes the system's rigid movement. The fast subsystem describes the system's flexible movement. Then, the appropriate controller is designed for each subsystem. The slow subsystem's controller $\boldsymbol{\tau}_{\mathrm{s}}$ is designed to achieve the desired trajectory asymptotic tracking. The fast subsystem's controller $\boldsymbol{\tau}_{\mathrm{f}}$ is designed to suppress the double vibration caused by the flexible joints and the flexible link [61]. So, we can write the system's total controller as: $\boldsymbol{\tau} = \boldsymbol{\tau}_{\mathrm{s}} + \boldsymbol{\tau}_{\mathrm{f}}$.

https://doi.org/10.1017/S0263574721000977 Published online by Cambridge University Press

First, we decomposed Eq. (10b) into the following form:

$$\begin{bmatrix} \boldsymbol{M}_{11} & \boldsymbol{M}_{12} & \boldsymbol{M}_{13} \\ \boldsymbol{M}_{21} & \boldsymbol{M}_{22} & \boldsymbol{M}_{23} \\ \boldsymbol{M}_{31} & \boldsymbol{M}_{32} & \boldsymbol{M}_{33} \end{bmatrix} \cdot \begin{bmatrix} \ddot{q}_0 \\ \ddot{\boldsymbol{q}}_\theta \\ \ddot{\boldsymbol{\delta}} \end{bmatrix} + \begin{bmatrix} N_1 \\ \boldsymbol{N}_2 \\ \boldsymbol{N}_3 \end{bmatrix} + \begin{bmatrix} 0 \\ -\boldsymbol{K}_\theta(\boldsymbol{\theta} - \boldsymbol{q}_\theta) \\ \boldsymbol{K}_\delta \boldsymbol{\delta} \end{bmatrix} = 0 \tag{11}$$

where $\boldsymbol{M}_{11} \in \boldsymbol{R}^{1\times1}, \boldsymbol{M}_{12} \in \boldsymbol{R}^{1\times2}, \boldsymbol{M}_{13} \in \boldsymbol{R}^{1\times2}, \boldsymbol{M}_{21} \in \boldsymbol{R}^{2\times1}, \boldsymbol{M}_{22} \in \boldsymbol{R}^{2\times2}, \boldsymbol{M}_{23} \in \boldsymbol{R}^{2\times2}, \boldsymbol{M}_{31} \in \boldsymbol{R}^{2\times1}, \boldsymbol{M}_{32} \in \boldsymbol{R}^{2\times2}$, and $\boldsymbol{M}_{33} \in \boldsymbol{R}^{2\times2}$ are the sub-matrices of $\boldsymbol{M}(\boldsymbol{q}, \boldsymbol{\delta})$. $\boldsymbol{N}_1 \in \boldsymbol{R}^{1\times1}, \boldsymbol{N}_2 \in \boldsymbol{R}^{2\times1}, \boldsymbol{N}_3 \in \boldsymbol{R}^{2\times1}$ are the sub-matrices of $\boldsymbol{H}(\boldsymbol{q}, \dot{\boldsymbol{q}}, \boldsymbol{\delta}, \dot{\boldsymbol{\delta}}) \begin{bmatrix} \dot{\boldsymbol{q}} \\ \dot{\boldsymbol{\delta}} \end{bmatrix}$.

From Eq. (11), we have

$$\ddot{q}_0 = -\boldsymbol{M}_{11}^{-1}(\boldsymbol{M}_{12}\ddot{\boldsymbol{q}}_\theta + \boldsymbol{M}_{13}\ddot{\boldsymbol{\delta}}) - \boldsymbol{M}_{11}^{-1}\boldsymbol{N}_1 \tag{12}$$

Substitute Eq. (12) into Eq. (11), we have

$$\begin{bmatrix} \boldsymbol{D}_{11} & \boldsymbol{D}_{12} \\ \boldsymbol{D}_{21} & \boldsymbol{D}_{22} \end{bmatrix} \cdot \begin{bmatrix} \ddot{\boldsymbol{q}}_\theta \\ \ddot{\boldsymbol{\delta}} \end{bmatrix} + \begin{bmatrix} \boldsymbol{C}_1 \\ \boldsymbol{C}_2 \end{bmatrix} + \begin{bmatrix} -\boldsymbol{K}_\theta(\boldsymbol{\theta} - \boldsymbol{q}_\theta) \\ \boldsymbol{K}_\delta \boldsymbol{\delta} \end{bmatrix} = 0 \tag{13}$$

where $\boldsymbol{D}_{11} = -\boldsymbol{M}_{21}\boldsymbol{M}_{11}^{-1}\boldsymbol{M}_{12} + \boldsymbol{M}_{22}$, $\boldsymbol{D}_{12} = -\boldsymbol{M}_{21}\boldsymbol{M}_{11}^{-1}\boldsymbol{M}_{13} + \boldsymbol{M}_{23}$, $\boldsymbol{D}_{21} = -\boldsymbol{M}_{31}\boldsymbol{M}_{11}^{-1}\boldsymbol{M}_{12} + \boldsymbol{M}_{32}$, $\boldsymbol{D}_{22} = -\boldsymbol{M}_{31}\boldsymbol{M}_{11}^{-1}\boldsymbol{M}_{13} + \boldsymbol{M}_{33}$, $\boldsymbol{C}_1 = -\boldsymbol{M}_{21}\boldsymbol{M}_{11}^{-1}\boldsymbol{N}_1 + \boldsymbol{N}_2$, $\boldsymbol{C}_2 = -\boldsymbol{M}_{31}\boldsymbol{M}_{11}^{-1}\boldsymbol{N}_1 + \boldsymbol{N}_3$.

Because the matrix $\begin{bmatrix} \boldsymbol{D}_{11} & \boldsymbol{D}_{12} \\ \boldsymbol{D}_{21} & \boldsymbol{D}_{22} \end{bmatrix}$ is symmetric and positive definite, it is reversible. Its inverse matrix can be expressed as:

$$\begin{bmatrix} \boldsymbol{D}_{11} & \boldsymbol{D}_{12} \\ \boldsymbol{D}_{21} & \boldsymbol{D}_{22} \end{bmatrix}^{-1} = \begin{bmatrix} \boldsymbol{G}_{11} & \boldsymbol{G}_{12} \\ \boldsymbol{G}_{21} & \boldsymbol{G}_{22} \end{bmatrix} \tag{14}$$

Let the flexible-joint error vector $\boldsymbol{\sigma} = \boldsymbol{\theta} - \boldsymbol{q}_\theta = [\,\sigma_1 \quad \sigma_2\,]^{\mathrm{T}}$. We rewrite Eqs. (10) and (13) as following

$$\ddot{\boldsymbol{\sigma}} = \ddot{\boldsymbol{\theta}} - \ddot{\boldsymbol{q}}_\theta = -\boldsymbol{J}_\theta^{-1}\boldsymbol{K}_\theta\sigma + \boldsymbol{J}_\theta^{-1}(\boldsymbol{\tau} + \boldsymbol{\tau}_{\mathrm{d}}) - \ddot{\boldsymbol{q}}_\theta \tag{15a}$$

$$\ddot{\boldsymbol{q}}_\theta = -\boldsymbol{G}_{11}\boldsymbol{C}_1 - \boldsymbol{G}_{12}\boldsymbol{C}_2 - \boldsymbol{G}_{12}\boldsymbol{K}_\delta\boldsymbol{\delta} + \boldsymbol{G}_{11}\boldsymbol{K}_\theta\boldsymbol{\sigma} \tag{15b}$$

$$\ddot{\boldsymbol{\delta}} = -\boldsymbol{G}_{21}\boldsymbol{C}_1 - \boldsymbol{G}_{22}\boldsymbol{C}_2 - \boldsymbol{G}_{22}\boldsymbol{K}_\delta\boldsymbol{\delta} + \boldsymbol{G}_{21}\boldsymbol{K}_\theta\boldsymbol{\sigma} \tag{15c}$$

Defining a singular perturbation factor: $\varepsilon^2 = 1/\min\{k_{\delta1}, k_{\delta2}, k_{\theta1}, k_{\theta2}\}$, two variables: $\boldsymbol{z}_\delta = \boldsymbol{\delta}/\varepsilon^2$ and $\boldsymbol{z}_\theta = \boldsymbol{\sigma}/\varepsilon^2$, two matrices: $\boldsymbol{K}_{\delta\varepsilon} = \varepsilon^2\boldsymbol{K}_\delta$ and $\boldsymbol{K}_{\theta\varepsilon} = \varepsilon^2\boldsymbol{K}_\theta$. Then, the singular perturbation model of the system's dynamic equation is established:

$$\varepsilon^2\ddot{\boldsymbol{z}}_\theta = -\boldsymbol{J}_\theta^{-1}\boldsymbol{K}_{\theta\varepsilon}\boldsymbol{z}_\theta + \boldsymbol{J}_\theta^{-1}(\boldsymbol{\tau} + \boldsymbol{\tau}_{\mathrm{d}}) - \ddot{\boldsymbol{q}}_\theta \tag{16a}$$

$$\ddot{\boldsymbol{q}}_\theta = -\boldsymbol{G}_{11}\boldsymbol{C}_1 - \boldsymbol{G}_{12}\boldsymbol{C}_2 - \boldsymbol{G}_{12}\boldsymbol{K}_{\delta\varepsilon}\boldsymbol{z}_\delta + \boldsymbol{G}_{11}\boldsymbol{K}_{\theta\varepsilon}\boldsymbol{z}_\theta \tag{16b}$$

$$\varepsilon^2\ddot{\boldsymbol{z}}_\delta = -\boldsymbol{G}_{21}\boldsymbol{C}_1 - \boldsymbol{G}_{22}\boldsymbol{C}_2 - \boldsymbol{G}_{22}\boldsymbol{K}_{\delta\varepsilon}\boldsymbol{z}_\delta + \boldsymbol{G}_{21}\boldsymbol{K}_{\theta\varepsilon}\boldsymbol{z}_\theta \tag{16c}$$

3.1. The slow subsystem

The slow subsystem only describes the system's rigid movement. So here, we can ignore the influences of the flexible joints and the flexible link. Let $\varepsilon = 0$, then Eq. (16) can be rewritten as:

$$0=-\boldsymbol{J}_{\theta}^{-1}\bar{\boldsymbol{K}}_{\theta\varepsilon}\bar{z}_{\theta}+\boldsymbol{J}_{\theta}^{-1}\left(\boldsymbol{\tau}_{s}+\boldsymbol{\tau}_{d}\right)-\ddot{\boldsymbol{q}}_{\theta} \tag{17a}$$

$$\ddot{\boldsymbol{q}}_{\theta}=-\bar{\boldsymbol{G}}_{11}\bar{C}_{1}-\bar{\boldsymbol{G}}_{12}\bar{C}_{2}-\bar{\boldsymbol{G}}_{12}\bar{\boldsymbol{K}}_{\delta\varepsilon}\bar{z}_{\delta}+\bar{\boldsymbol{G}}_{11}\bar{\boldsymbol{K}}_{\theta\varepsilon}\bar{z}_{\theta} \tag{17b}$$

$$0=-\bar{\boldsymbol{G}}_{21}\bar{C}_{1}-\bar{\boldsymbol{G}}_{22}\bar{C}_{2}-\bar{\boldsymbol{G}}_{22}\bar{\boldsymbol{K}}_{\delta\varepsilon}\bar{z}_{\delta}+\bar{\boldsymbol{G}}_{21}\bar{\boldsymbol{K}}_{\theta\varepsilon}\bar{z}_{\theta} \tag{17c}$$

where $\bar{\boldsymbol{A}}$ is the corresponding matrix or variable of $\boldsymbol{A}$ when $\varepsilon=0$, that is, the corresponding matrix or variable calculated in the slowly varying time scale.

From Eq. (17a)

$$\bar{z}_{\theta}=\bar{\boldsymbol{K}}_{\theta\varepsilon}^{-1}(\boldsymbol{\tau}_{s}+\boldsymbol{\tau}_{d}-\boldsymbol{J}_{\theta}\ddot{\boldsymbol{q}}_{\theta}) \tag{18}$$

Substituting Eq. (18) into Eq. (17c), we can get:

$$\bar{z}_{\delta}=\bar{\boldsymbol{K}}_{\delta\varepsilon}^{-1}\bar{\boldsymbol{G}}_{22}^{-1}[-\bar{\boldsymbol{G}}_{21}\bar{\boldsymbol{C}}_{1}-\bar{\boldsymbol{G}}_{22}\bar{\boldsymbol{C}}_{2}+\bar{\boldsymbol{G}}_{21}(\boldsymbol{\tau}_{s}+\boldsymbol{\tau}_{d}-\boldsymbol{J}_{\theta}\ddot{\boldsymbol{q}}_{\theta})] \tag{19}$$

Then, substituting Eqs. (18) and (19) into Eq. (17b), the slow subsystem's dynamics equation can be obtained as:

$$\boldsymbol{D}_{s}\ddot{\boldsymbol{q}}_{\theta}+\boldsymbol{C}_{s}=\boldsymbol{\tau}_{s}+\boldsymbol{\tau}_{d} \tag{20}$$

where $\boldsymbol{D}_{s}=[\bar{\boldsymbol{G}}_{11}-\bar{\boldsymbol{G}}_{12}\bar{\boldsymbol{G}}_{22}^{-1}\bar{\boldsymbol{G}}_{21}]^{-1}+J_{\theta}$, $\boldsymbol{C}_{s}=[\bar{\boldsymbol{G}}_{11}-\bar{\boldsymbol{G}}_{12}\bar{\boldsymbol{G}}_{22}^{-1}\bar{\boldsymbol{G}}_{21}]^{-1}(\bar{\boldsymbol{G}}_{11}-\bar{\boldsymbol{G}}_{12})\cdot\boldsymbol{C}_{1}$.

Equation (20) can be rewritten as a quasi-linear form:

$$\boldsymbol{D}_{s}\ddot{\boldsymbol{q}}_{\theta}+\boldsymbol{H}_{s}\dot{\boldsymbol{q}}_{\theta}=\boldsymbol{\tau}_{s}+\boldsymbol{\tau}_{d} \tag{21}$$

where $\boldsymbol{H}_{s}\in\boldsymbol{R}^{2\times2}$ is not unique, but it can satisfy [62]

$$\boldsymbol{x}^{T}(\dot{\boldsymbol{D}}_{s}-2\boldsymbol{H}_{s})\boldsymbol{x}=0,\quad\forall\boldsymbol{x}\in\boldsymbol{R}^{2\times1} \tag{22}$$

Considering the system's uncertainty,

$$\boldsymbol{D}_{s}=\hat{\boldsymbol{D}}_{s}+\Delta\boldsymbol{D}_{s},\quad\boldsymbol{H}_{s}=\hat{\boldsymbol{H}}_{s}+\Delta\boldsymbol{H}_{s} \tag{23}$$

where $\hat{\boldsymbol{D}}_{s}$ and $\hat{\boldsymbol{H}}_{s}$ are the approximate matrices of $\boldsymbol{D}_{s}$ and $\boldsymbol{H}_{s}$, respectively, and $\Delta\boldsymbol{D}_{s}$ and $\Delta\boldsymbol{H}_{s}$ are the system model estimation errors.

Assuming the system's uncertain parameters are bounded, $\Delta\boldsymbol{D}_{s}$ and $\Delta\boldsymbol{H}_{s}$ are also bounded. There are positive constants l_{d} and l_{h},

$$\|\Delta\boldsymbol{D}_{s}\|\leq\mathrm{l}_{d},\quad\|\Delta\boldsymbol{H}\|\leq l_{h}\;\|\dot{\boldsymbol{q}}\| \tag{24}$$

And, assuming $\boldsymbol{\tau}_{d}$ is bounded. So, there is a positive constant l_{t} that satisfies:

$$\|\boldsymbol{\tau}_{d}\|\leq l_{t} \tag{25}$$

Defined $\boldsymbol{q}_{d}=[\,q_{1d}\quad q_{2d}\,]^{T}$ be the expected output vector of the slow subsystem, then the output error vector $\boldsymbol{e}$ between $\boldsymbol{q}_{d}$ and the actual output vector $\boldsymbol{q}_{\theta}=[\,q_{1}\quad q_{2}\,]^{T}$ is: $\boldsymbol{e}=\boldsymbol{q}_{\theta}-\boldsymbol{q}_{d}=[\,e_{1}\quad e_{2}\,]^{T}$.

Selecting the following sliding surface

$$\boldsymbol{s}=\dot{\boldsymbol{e}}+\lambda\boldsymbol{e} \tag{26}$$

where λ is a positive constant diagonal matrix.

Derivating $\boldsymbol{s}$

$$\dot{\boldsymbol{s}}=\ddot{\boldsymbol{e}}+\lambda\dot{\boldsymbol{e}}=\ddot{\boldsymbol{q}}_{\theta}-\ddot{\boldsymbol{q}}_{\theta d}+\lambda\dot{\boldsymbol{e}} \tag{27}$$

Substitute Eq. (16a) into Eq. (12),

$$\boldsymbol{D}_{s}\dot{\boldsymbol{s}}=\boldsymbol{\tau}_{s}+\boldsymbol{\tau}_{d}-\boldsymbol{H}_{s}\dot{\boldsymbol{q}}_{\theta}-\boldsymbol{D}_{s}\ddot{\boldsymbol{q}}_{\theta d}+\boldsymbol{D}_{s}\lambda\dot{\boldsymbol{e}} \tag{28}$$

The slow subsystem's controller is designed as follows:

$$\boldsymbol{\tau}_{s}=\boldsymbol{u}_{1}+\boldsymbol{u}_{2}+\boldsymbol{u}_{3} \tag{29}$$

https://doi.org/10.1017/S0263574721000977 Published online by Cambridge University Press

(1) $\boldsymbol{u}_1$ is an equivalent controller,

$$\boldsymbol{u}_1 = \hat{\boldsymbol{D}}_{\mathrm{s}}\ddot{\boldsymbol{q}}_{\theta\mathrm{d}} + \hat{\boldsymbol{H}}_{\mathrm{s}}\dot{\boldsymbol{q}}_{\theta} - \hat{\boldsymbol{D}}_{\mathrm{s}}\lambda\dot{\boldsymbol{e}} - \hat{\boldsymbol{H}}_{\mathrm{s}}\boldsymbol{s} \tag{30}$$

(2) $\boldsymbol{u}_2$ is a robust controller. It is used to compensate for the system's uncertain parameter and external disturbance.

$$\boldsymbol{u}_2 = -\boldsymbol{K}_{\mathrm{s}}\mathbf{sat}\left(\frac{\boldsymbol{s}}{\boldsymbol{\Phi}}\right) \tag{31}$$

where $\boldsymbol{K}_{\mathrm{s}} = l_{\mathrm{d}}\left\|\lambda\dot{\boldsymbol{e}} - \ddot{\boldsymbol{q}}_{\theta\mathrm{d}}\right\| + l_{\mathrm{h}}\left\|\dot{\boldsymbol{q}}_{\theta}\right\| \cdot \left\|\boldsymbol{s} - \dot{\boldsymbol{q}}_{\theta}\right\| + l_{\mathrm{t}}$. $\mathbf{sat}(\frac{\boldsymbol{s}}{\boldsymbol{\Phi}}) = \left[\,\mathrm{sat}(\frac{s_1}{\Phi_1}) \quad \mathrm{sat}(\frac{s_2}{\Phi_2})\,\right]^{\mathrm{T}}$, it is a saturated function vector. It is used to reduce the chattering of sliding mode control itself, its elements are:

$$\mathrm{sat}\left(\frac{s_i}{\Phi_i}\right) = \begin{cases} \mathrm{sgn}(s_i) & \text{if } |s_i| > \Phi_i \\ \frac{s_i}{\Phi_i} & \text{if } |s_i| \le \Phi_i \end{cases}, \quad (i = 1, 2) \tag{32}$$

where $\Phi = \left[\,\boldsymbol{\Phi}_1 \quad \Phi_2\,\right]^{\mathrm{T}}$, Φ_1 and Φ_2 are positive parameters, s_i is the i th element of $\boldsymbol{s}$, and Φ_i is the i th element of $\boldsymbol{\Phi}$.

(3) $\boldsymbol{u}_3$ is a fuzzy controller. It is used to reduce the vibration of sliding mode control, improve the approach speed, and ensure the system's stability.

$\boldsymbol{u}_3$ is designed based on the results of the system stability analysis, as follows:

Defined a Lyapunov function:

$$\boldsymbol{V} = \frac{1}{2}s^{\mathrm{T}}D_{\mathrm{s}}s \tag{33}$$

Differentiating $\boldsymbol{V}$, and combining Eqs. (22) and (28), then

$$\dot{\boldsymbol{V}} = \boldsymbol{s}^{\mathrm{T}}\boldsymbol{D}_{\mathrm{s}}\dot{\boldsymbol{s}} + \frac{1}{2}\boldsymbol{s}^{\mathrm{T}}\dot{\boldsymbol{D}}_{\mathrm{s}}\boldsymbol{s} = \boldsymbol{s}^{\mathrm{T}}(\boldsymbol{\tau}_{\mathrm{s}} + \boldsymbol{\tau}_{\mathrm{d}} - \boldsymbol{H}_{\mathrm{s}}\dot{\boldsymbol{q}}_{\theta} - \boldsymbol{D}_{\mathrm{s}}\ddot{\boldsymbol{q}}_{\theta\mathrm{d}} + \boldsymbol{D}_{\mathrm{s}}\lambda\dot{\boldsymbol{e}}) + \boldsymbol{s}^{\mathrm{T}}\boldsymbol{H}_{\mathrm{s}}\boldsymbol{s} \tag{34}$$

Substitute Eqs. (23), (29), (30), and (31) into Eq. (34), we have

$$\begin{aligned}\dot{\boldsymbol{V}} &= \boldsymbol{s}^{\mathrm{T}}[\hat{\boldsymbol{D}}_{\mathrm{s}}\ddot{\boldsymbol{q}}_{\theta\mathrm{d}} + \hat{\boldsymbol{H}}_{\mathrm{s}}\dot{\boldsymbol{q}}_{\theta} - \hat{\boldsymbol{D}}_{\mathrm{s}}\lambda\dot{\boldsymbol{e}} - \hat{\boldsymbol{H}}_{\mathrm{s}}\boldsymbol{s} - \boldsymbol{K}_{\mathrm{s}}\mathrm{sat}\left(\frac{\boldsymbol{s}}{\boldsymbol{\Phi}}\right) + \boldsymbol{u}_3 + \boldsymbol{\tau}_{\mathrm{d}} - \boldsymbol{H}_{\mathrm{s}}\dot{\boldsymbol{q}}_{\theta} - \boldsymbol{D}_{\mathrm{s}}\ddot{\boldsymbol{q}}_{\theta\mathrm{d}} + \boldsymbol{D}_{\mathrm{s}}\lambda\dot{\boldsymbol{e}}] + \boldsymbol{s}^{\mathrm{T}}\boldsymbol{H}_{\mathrm{s}}\boldsymbol{s} \\ &= \boldsymbol{s}^{\mathrm{T}}\left[\Delta\boldsymbol{D}_{\mathrm{s}}\left(\lambda\dot{\boldsymbol{e}} - \ddot{\boldsymbol{q}}_{\theta\mathrm{d}}\right) + \Delta\boldsymbol{H}_{\mathrm{s}}(\boldsymbol{s} - \dot{\boldsymbol{q}}_{\theta}) - \boldsymbol{K}_{\mathrm{s}}\mathbf{sat}\left(\frac{\boldsymbol{s}}{\boldsymbol{\Phi}}\right) + \boldsymbol{u}_3 + \boldsymbol{\tau}_{\mathrm{d}}\right]\end{aligned} \tag{35}$$

The system's stability analysis has two cases:

Case 1: when $|s_i| > \Phi_i$, $sat(\frac{s_i}{\Phi_i}) = \mathrm{sgn}(s_i)$. Substitute (24) and (25) into Eq. (35), we have:

$$\dot{\boldsymbol{V}} \le \boldsymbol{s}^{\mathrm{T}}\boldsymbol{u}_3 \tag{36}$$

So when $\boldsymbol{s}^{\mathrm{T}}\boldsymbol{u}_3 < 0$, $\dot{\boldsymbol{V}} < 0$. Thus, the asymptotic stability of $\boldsymbol{s}, \boldsymbol{e}, \dot{\boldsymbol{e}}$ outside the boundary layer can be guaranteed.

Case 2: when $|s_i| \le \Phi_i$, $\mathrm{sat}(\frac{s_i}{\Phi_i}) = \frac{s_i}{\Phi_\mathrm{i}}$. Substitute (24) and (25) into Eq. (35), we have:

$$\begin{aligned}\dot{\boldsymbol{V}} &\le \boldsymbol{s}^{\mathrm{T}}\left(\mathrm{l}_{\mathrm{d}}\left\|\lambda\dot{\boldsymbol{e}} - \ddot{\boldsymbol{q}}_{\theta\mathrm{d}}\right\| + \mathrm{l}_{\mathrm{h}}\left\|\dot{\boldsymbol{q}}_{\theta}\right\| \cdot \left\|\boldsymbol{s} - \dot{\boldsymbol{q}}_{\theta}\right\| - \boldsymbol{K}_{\mathrm{s}}\frac{\boldsymbol{s}}{\boldsymbol{\Phi}} + \boldsymbol{u}_3 + \mathrm{l}_{\mathrm{t}}\right) \\ &\le l_{\mathrm{d}}\left\|\lambda\dot{\boldsymbol{e}} - \ddot{\boldsymbol{q}}_{\theta\mathrm{d}}\right\| \cdot \|\boldsymbol{s}\| + l_{\mathrm{h}}\|\dot{q}_{\theta}\| \cdot \left\|\boldsymbol{s} - \dot{\boldsymbol{q}}_{\theta}\right\| \cdot \|\boldsymbol{s}\| - \boldsymbol{K}_{\mathrm{s}}\frac{\|\boldsymbol{s}\|^2}{\|\boldsymbol{\Phi}\|} + \boldsymbol{s}^{\mathrm{T}}\boldsymbol{u}_3 + l_{\mathrm{t}}\|\boldsymbol{s}\| \\ &= \left(l_{\mathrm{d}}\left\|\lambda\dot{\boldsymbol{e}} - \ddot{\boldsymbol{q}}_{\theta\mathrm{d}}\right\| + l_{\mathrm{h}}\left\|\dot{\boldsymbol{q}}_{\theta}\right\| \cdot \left\|\boldsymbol{s} - \dot{\boldsymbol{q}}_{\theta}\right\| + l_{\mathrm{t}}\right) \cdot \|\boldsymbol{s}\| - \boldsymbol{K}_{\mathrm{s}}\frac{\|\boldsymbol{s}\|^2}{\|\boldsymbol{\Phi}\|} + \boldsymbol{s}^{\mathrm{T}}\boldsymbol{u}_3 \\ &= \boldsymbol{K}_{\mathrm{s}}\left(\|\boldsymbol{s}\| - \frac{\|\boldsymbol{s}\|^2}{\|\boldsymbol{\Phi}\|}\right) + \boldsymbol{s}^{\mathrm{T}}\boldsymbol{u}_3\end{aligned} \tag{37}$$

So when $\boldsymbol{s}^{\mathrm{T}}\boldsymbol{u}_3 \le -\boldsymbol{K}_{\mathrm{s}}(\,\|\boldsymbol{s}\| - \frac{\|\boldsymbol{s}\|^2}{\|\boldsymbol{\Phi}\|})$, $\dot{\boldsymbol{V}} \le 0$, and $\lim\limits_{t\to 0} \boldsymbol{s} = 0$.

Table I. *The fuzzy rules.*

s	NB	NM	NS	ANZ	APZ	PS	PM	PB
u_3	PS	PM	PB	PB	NB	NB	NM	NS

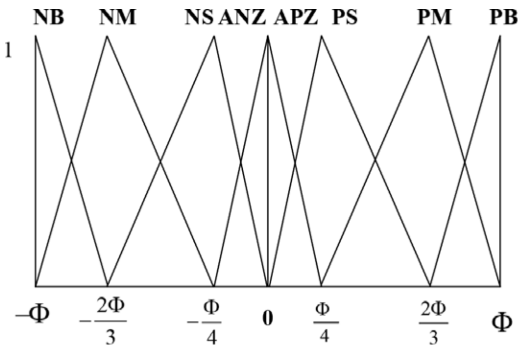

Figure 3. *Membership function of* $\boldsymbol{s}$.

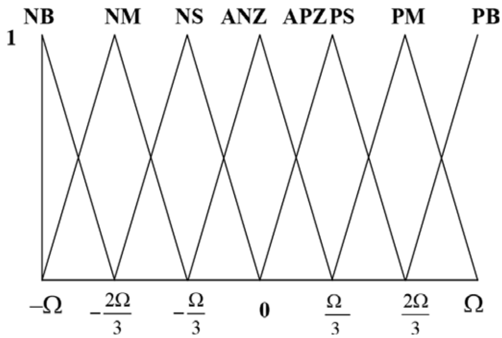

Figure 4. *Membership function of* $\boldsymbol{u}_3$.

In conclusion, when $\boldsymbol{s}^{\mathrm{T}}\boldsymbol{u}_3 < 0$ and $\boldsymbol{s}^{\mathrm{T}}\boldsymbol{u}_3 \leq -\boldsymbol{K}_{\mathrm{s}}(\ \|\boldsymbol{s}\| - \frac{\|s\|^2}{\|\Phi\|})$, $\dot{V} \leq 0$, $\boldsymbol{s}$, $\boldsymbol{e}$, $\dot{\boldsymbol{e}}$ are asymptotically stable.

To satisfy the above conditions, a one-input one-output fuzzy controller is designed. The input variable is $\boldsymbol{s}$, and the output variable is $\boldsymbol{u}_3$. The membership function of the input variable $\boldsymbol{s}$ is shown in Fig. 3. The membership function of output variables $\boldsymbol{u}_3$ is shown in Fig. 4. Where Φ is the design parameter defined in Eq. (32), Ω is a new design parameter which can be selected by trial and experience. The fuzzy controller's working principle is: $\boldsymbol{u}_3$ can be chosen appropriately according to $\boldsymbol{s}$'s value to satisfy the requirements of system control. The fuzzy base rule is shown in Table I in which the following abbreviations have been used: NB: Negative Big; NM: Negative Medium; NS: Negative Small; ANZ: Approach Negative Zero; APZ: Approach Positive Zero; PS: Positive Small; PM: Positive Medium; PB: Positive Big. For example, when $\boldsymbol{s}$ is NB, $\boldsymbol{u}_3$ is PS; when $\boldsymbol{s}$ is NM, $\boldsymbol{u}_3$ is PM. Finally, we use the center of gravity method to solve the fuzzy problem.

3.2. The fast subsystem

The fast subsystem describes the system's flexible movement. The flexible joints and the flexible link will not only affect the control but also produce vibration. And, their vibration levels are not the same. So, we further decompose the fast subsystem into two independent sub-sub systems: the flexible-joint fast subsystem and the flexible-link fast subsystem. The flexible-joint fast subsystem describes the system's flexible movement caused by the flexible joints. And, the flexible-link fast subsystem describes

https://doi.org/10.1017/S0263574721000977 Published online by Cambridge University Press

the system's flexible movement caused by the flexible link. The flexible-joint fast subsystem's controller τ_{f1} is designed to suppress the vibration caused by the flexible joints. The flexible-link fast subsystem's controller $\boldsymbol{\tau}_{f2}$ is used to suppress the vibration caused by the flexible-link actively. So, the total controller for the fast subsystem is: $\boldsymbol{\tau}_f = \boldsymbol{\tau}_{f1} + \boldsymbol{\tau}_{f2}$.

3.2.1. The flexible-joint fast subsystem

Now, only the influence of the flexible joints is considered. So, let $\boldsymbol{\delta} = 0$ in Eq. (16), the dynamic equation of the rigid-link and flexible-joints system is obtained as:

$$\varepsilon^2 \ddot{z}_\theta = -\boldsymbol{J}_\theta^{-1} \boldsymbol{K}_{\theta\varepsilon} z_\theta + \boldsymbol{J}_\theta^{-1} \boldsymbol{\tau}_{k1} - \ddot{\boldsymbol{q}}_\theta \tag{38a}$$

$$\ddot{\boldsymbol{q}}_\theta = -\boldsymbol{D}_s^{-1} \left(\boldsymbol{C}_1 - \boldsymbol{K}_{\theta\varepsilon} z_\theta \right) \tag{38b}$$

where $\boldsymbol{\tau}_{k1} = \boldsymbol{\tau}_s + \boldsymbol{\tau}_{f1} + \boldsymbol{\tau}_d$.

The feedback controller is designed as following

$$\boldsymbol{\tau}_{f1} = \frac{\boldsymbol{K}_f(\dot{\boldsymbol{q}}_\theta - \dot{\boldsymbol{\theta}})}{\varepsilon^2} \tag{39}$$

where $\boldsymbol{K}_f = \boldsymbol{K}_2/\varepsilon^2$, $\boldsymbol{K}_2$ is a positive definite diagonal matrix.

The controller can adjust $\boldsymbol{K}_f$ in time according to the difference of the link's rotation angular velocity $\dot{\boldsymbol{q}}_\theta$ and the motor rotor's rotation angular velocity $\dot{\boldsymbol{\theta}}$. The stability of the flexible-joint fast subsystem is ensured. Combining with Eq. (38), the flexible-joint fast subsystem's dynamic equation is:

$$\varepsilon^2 \ddot{\boldsymbol{z}}_\theta = \boldsymbol{J}_\theta^{-1}(\boldsymbol{\tau}_s + \boldsymbol{\tau}_d - \boldsymbol{K}_{\theta\varepsilon} z_\theta - \boldsymbol{J}_\theta \ddot{\boldsymbol{q}}_\theta) - \varepsilon^2 \boldsymbol{J}_\theta^{-1} \boldsymbol{K}_2 \dot{\boldsymbol{z}}_\theta \tag{40}$$

3.2.2. The flexible-link fast subsystem

Now, only the influence of the flexible link is considered. So let $\boldsymbol{\theta} = \boldsymbol{q}_\theta$, $\dot{\boldsymbol{\theta}} = \dot{\boldsymbol{q}}_\theta$ in Eq. (16), the dynamic equation of the flexible-link and rigid-joints system is obtained as:

$$\ddot{\boldsymbol{q}}_\theta = -\boldsymbol{G}_{11}^* \boldsymbol{C}_1 - \boldsymbol{G}_{12}^* \boldsymbol{C}_2 - \boldsymbol{G}_{12}^* K_{\delta\varepsilon} z_\delta + \boldsymbol{G}_{11}^* \boldsymbol{\tau}_{k2} \tag{41a}$$

$$\varepsilon^2 \ddot{\boldsymbol{z}}_\delta = -\boldsymbol{G}_{21}^* \boldsymbol{C}_1 - \boldsymbol{G}_{22}^* \boldsymbol{C}_2 - \boldsymbol{G}_{22}^* K_{\delta\varepsilon} z_\delta + \boldsymbol{G}_{21}^* \boldsymbol{\tau}_{k2} \tag{41b}$$

where $\boldsymbol{\tau}_{k2} = \boldsymbol{\tau}_s + \boldsymbol{\tau}_{f2} + \boldsymbol{\tau}_d$, $\boldsymbol{G}_{11}^* = \left(\begin{bmatrix} 1 & 0 \\ 0 & 1 \end{bmatrix} + \boldsymbol{G}_{11} J_\theta \right)^{-1} \boldsymbol{G}_{11}$, $\boldsymbol{G}_{12}^* = \left(\begin{bmatrix} 1 & 0 \\ 0 & 1 \end{bmatrix} + \boldsymbol{G}_{11} J_\theta \right)^{-1} \boldsymbol{G}_{12}$, $\boldsymbol{G}_{21}^* = \boldsymbol{G}_{21} - \left(\begin{bmatrix} 1 & 0 \\ 0 & 1 \end{bmatrix} + \boldsymbol{G}_{11} J_\theta \right)^{-1} \boldsymbol{G}_{21} J_\theta \boldsymbol{G}_{11}$, $\boldsymbol{G}_{22}^* = \boldsymbol{G}_{22} - \left(\begin{bmatrix} 1 & 0 \\ 0 & 1 \end{bmatrix} + \boldsymbol{G}_{11} J_\theta \right)^{-1} \boldsymbol{G}_{21} J_\theta \boldsymbol{G}_{12}$.

Definite a fast time variant: $\boldsymbol{t}_f = \boldsymbol{t}/\varepsilon^2$, and its modifications: $z_{f1} = z_\delta - \bar{z}_\delta$ and $z_{f2} = \varepsilon^2 \dot{z}_\delta$. In the fast subsystem, the slow variables can be regarded as constants, that is, $\mathrm{d}\bar{z}_\delta/\mathrm{d}t_f = \varepsilon^2 \dot{\bar{z}}_\delta = 0$. Let $\varepsilon = 0$, the dynamic equation of the flexible-link fast subsystem can be obtained as:

$$\frac{\mathrm{d}\boldsymbol{Z}_f}{\mathrm{d}t_f} = \boldsymbol{A}_f \boldsymbol{Z}_f + \boldsymbol{B}_f \boldsymbol{\tau}_{f2} \tag{42}$$

where $\boldsymbol{Z}_f = \begin{bmatrix} z_{f1} \\ z_{f2} \end{bmatrix}$, $\boldsymbol{A}_f = \begin{bmatrix} 0 & \boldsymbol{I} \\ -\bar{\boldsymbol{G}}_{22}^* \boldsymbol{K}_{\delta\varepsilon} & 0 \end{bmatrix}$, $\mathbf{B}_f = \begin{bmatrix} 0 \\ \bar{\boldsymbol{G}}_{21}^* \end{bmatrix}$.

Because Eq. (42) is linear controlled, we can adjust the system state variable $\boldsymbol{Z}_f$ using a linear-quadratic optimal controller. It can reach zero to realize the active suppression of the elastic

https://doi.org/10.1017/S0263574721000977 Published online by Cambridge University Press

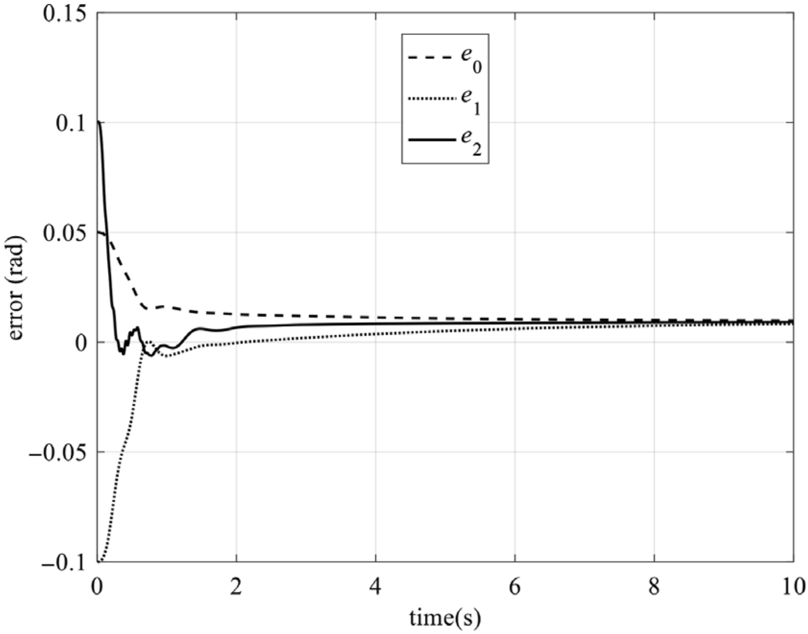

Figure 5. *The space manipulator trajectory tracking errors.*

vibration caused by the flexible link. Choosing the performance function of the optimal control: $\boldsymbol{J}_{\mathrm{f}} = \frac{1}{2}\int_0^{\infty}(\boldsymbol{Z}_{\mathrm{f}}^{\mathrm{T}}\boldsymbol{Q}_{\mathrm{f}}\boldsymbol{Z}_{\mathrm{f}} + \boldsymbol{\tau}_{\mathrm{f2}}^{\mathrm{T}}\boldsymbol{R}_{\mathrm{f}}\boldsymbol{\tau}_{\mathrm{f2}})\mathrm{d}\boldsymbol{t}_{\mathrm{f}}$, the controller can be designed as:

$$\boldsymbol{\tau}_{\mathrm{f2}} = -\boldsymbol{R}_{\mathrm{f}}^{-1}\boldsymbol{B}_{\mathrm{f}}^{\mathrm{T}}\boldsymbol{P}\boldsymbol{Z}_{\mathrm{f}} \tag{43}$$

where $\boldsymbol{Q}_{\mathrm{f}}$ and $\boldsymbol{R}_{\mathrm{f}}$ are symmetric positive definite matrices; $\boldsymbol{P}$ is the only solution for the Ricatti equation [63]: $\boldsymbol{P}\boldsymbol{A}_f + \boldsymbol{A}_f^T\boldsymbol{P} - \boldsymbol{P}\boldsymbol{B}_f\boldsymbol{R}_f^{-1}\boldsymbol{B}_f^T\boldsymbol{P} + \boldsymbol{Q}_f = 0$.

4. Simulation

We use the proposed hybrid controller to simulate the free-floating flexible-joints and flexible-link space manipulator system shown in Fig. 1. The actual values of the parameters in the system are: $m_0 = 40\mathrm{kg}$, $m_1 = 2\mathrm{kg}$, $\rho = 1\mathrm{kg/m}$, $l_1 = 3\mathrm{m}$, $l_2 = 3\mathrm{m}$, $EI = 300\mathrm{N}\cdot\mathrm{m}^2$, $J_0 = 34.17\mathrm{kg}\cdot\mathrm{m}^2$, $J_1 = 3\mathrm{kg}\cdot\mathrm{m}^2$, $J_{\theta 1} = J_{\theta 2} = 0.5\mathrm{kg}\cdot\mathrm{m}^2$, $k_{\theta 1} = k_{\theta 2} = 300\mathrm{N}\cdot\mathrm{m/rad}$. The flexible link is easy to deform, so l_2 is uncertain. In the simulation, its estimated value is: $l_2 = 2.5\mathrm{m}$. The fuzzy parameters are: $\Phi_1 = \Phi_2 = 1$, $\Omega_1 = \Omega_2 = 10$. The control parameters are: $\lambda = diag(12, 12)$, $l_{\mathrm{d}} = 1$, $l_{\mathrm{h}} = 1$, $l_t = 2$, $\boldsymbol{K}_2 = \mathrm{diag}(100, 100)$, $\boldsymbol{Q}_f = \mathrm{diag}(0.1, 0.1)$, $\boldsymbol{R}_f = \mathrm{diag}(0.01, 0.01)$.

Simulation 1:

First, a simple simulation is taken. The desired trajectories are: $q_{0\mathrm{d}} = 0$, $q_{1\mathrm{d}} = 0.1\mathrm{rad}$, $q_{2\mathrm{d}} = 0$. The initial states are: $\boldsymbol{q}(0) = \begin{bmatrix} 0.05 & 0 & 0.1 \end{bmatrix}^{\mathrm{T}}\mathrm{rad}$, $\boldsymbol{\theta}(0) = \begin{bmatrix} 0 & 0.1 \end{bmatrix}^{\mathrm{T}}\mathrm{rad}$, $\boldsymbol{\delta}\,(0) = \begin{bmatrix} 0 & 0 \end{bmatrix}^{\mathrm{T}} m$. The simulation time: $t = 10\mathrm{s}$. None external interference signal.

The simulation results are shown in Figs. 5–8. Figure 5 is the space manipulator trajectory tracking error curve. Figure 6 is the curve of the flexible link's mode coordinate. Figure 7 is the flexible link's deformation curve. Figure 8 shows the flexible-joints angle errors. We can see that the system's trajectory tracking errors converge to zero (the error is only 0.009 rad). The flexible-link's vibration is suppressed, and its deformation is compensated. The flexible-joints angle errors are decreased. The control is effective.

https://doi.org/10.1017/S0263574721000977 Published online by Cambridge University Press

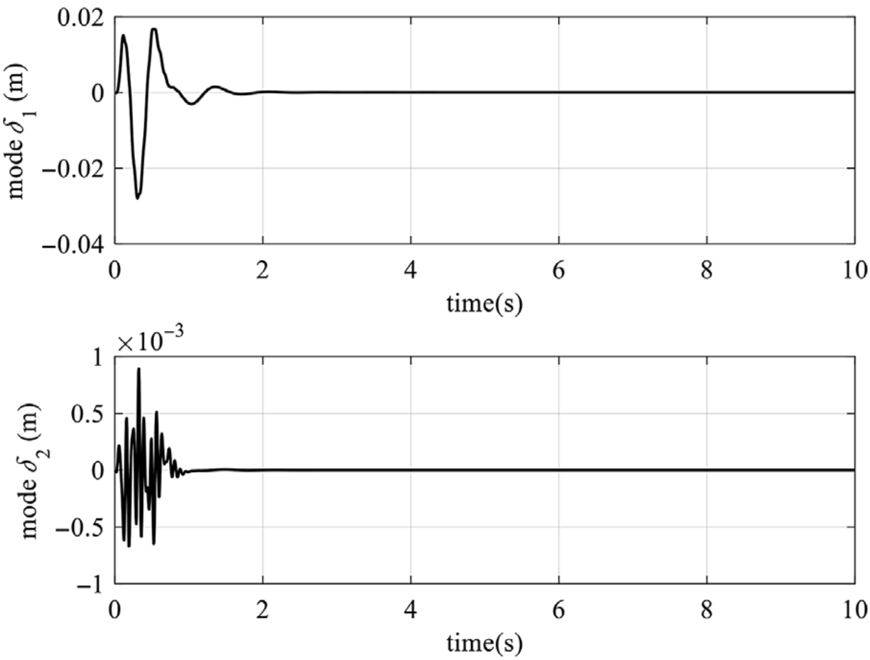

Figure 6. *The flexible link's mode coordinate.*

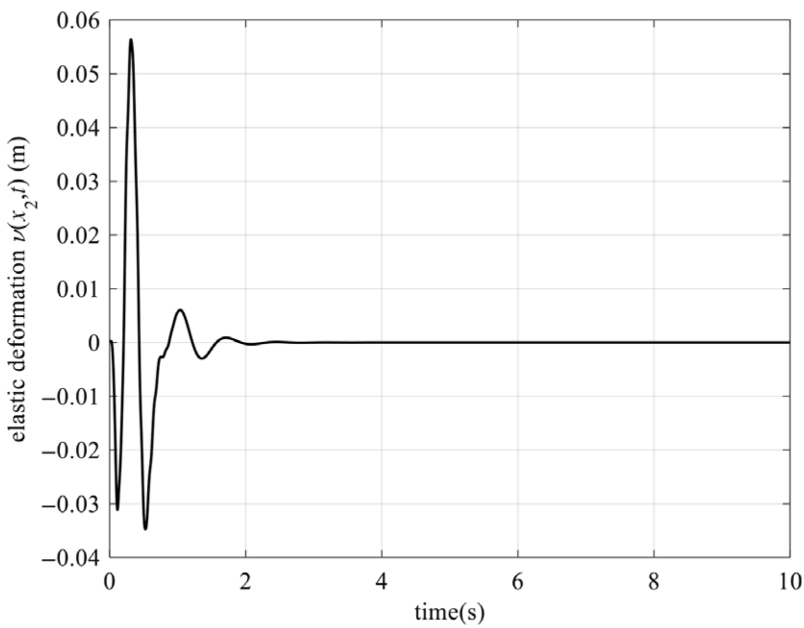

Figure 7. *The flexible link's deformation.*

But, the desired trajectories are simple, and the external interference is not considered in simulation 1. So, simulation 2 is taken.

Simulation 2:

The desired trajectories are: $q_{0d} = \frac{\pi}{4}\left[\frac{t}{10} - \frac{1}{2\pi}\sin\left(\frac{\pi}{5}t\right)\right]$, $q_{1d} = \frac{\pi}{2}\left[\frac{t}{10} - \frac{1}{2\pi}\sin\left(\frac{\pi}{5}t\right)\right]$, $q_{2d} = \frac{\pi}{2}\left[1 - \frac{t}{10} + \frac{1}{2\pi}\sin\left(\frac{\pi}{5}t\right)\right]$. The initial state is: $\boldsymbol{q}(0) = [0 \quad 0.1 \quad 1.5]^{\mathrm{T}}$rad, $\boldsymbol{\theta}(0) = [0.1 \quad 1.5]^{\mathrm{T}}$rad,

https://doi.org/10.1017/S0263574721000977 Published online by Cambridge University Press

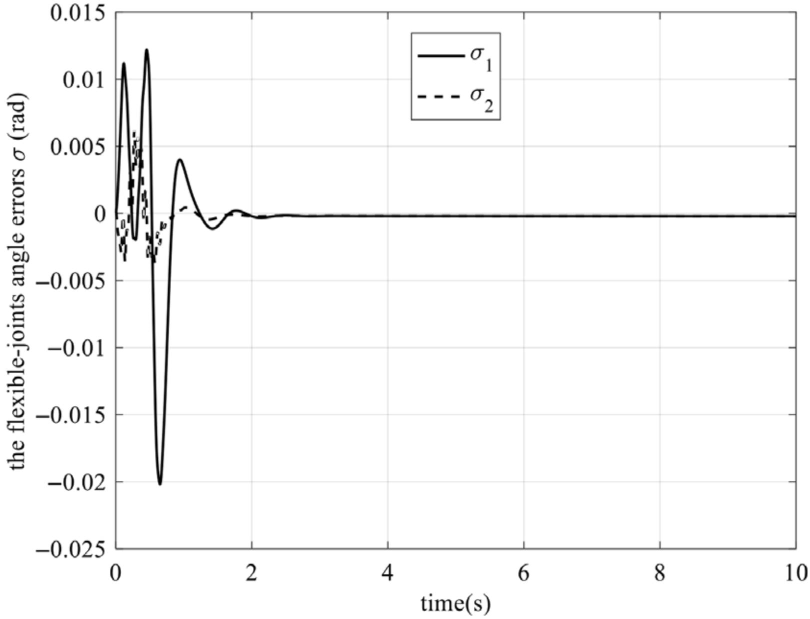

Figure 8. *The flexible-joints angle errors σ.*

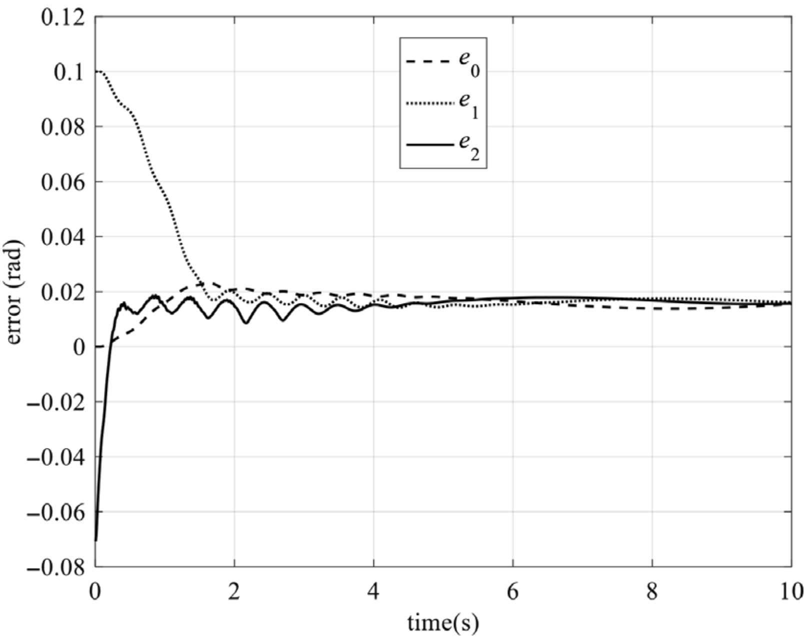

Figure 9. *The space manipulator trajectory tracking errors.*

$\boldsymbol{\delta}(0) = [0 \quad 0]^{\mathrm{T}} m$. The simulation time: $\mathrm{t} = 10\mathrm{s}$. The external interference signal is: $\boldsymbol{\tau}_{\mathrm{d}} = \left[\sin(\mathrm{t}) \quad \cos(\mathrm{t})\right]^{\mathrm{T}} \mathrm{N} \cdot \mathrm{m}$.

The simulation results are shown in Figs. 9–12. Figure 9 is the space manipulator trajectory tracking error curve. Figure 10 is the curve of the flexible link's mode coordinate. Figure 11 is the flexible link's deformation curve. Figure 12 shows the flexible-joints angle errors. The results show that the system

https://doi.org/10.1017/S0263574721000977 Published online by Cambridge University Press

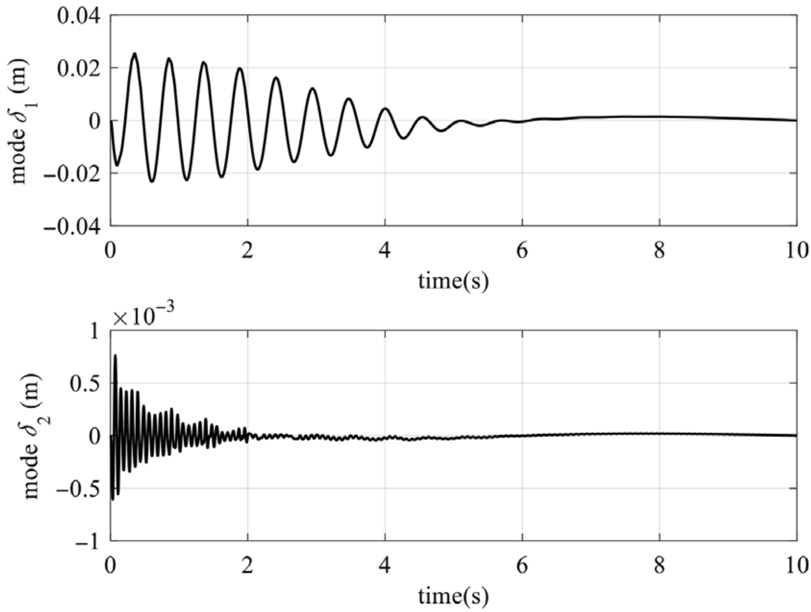

Figure 10. *The flexible link's mode coordinate.*

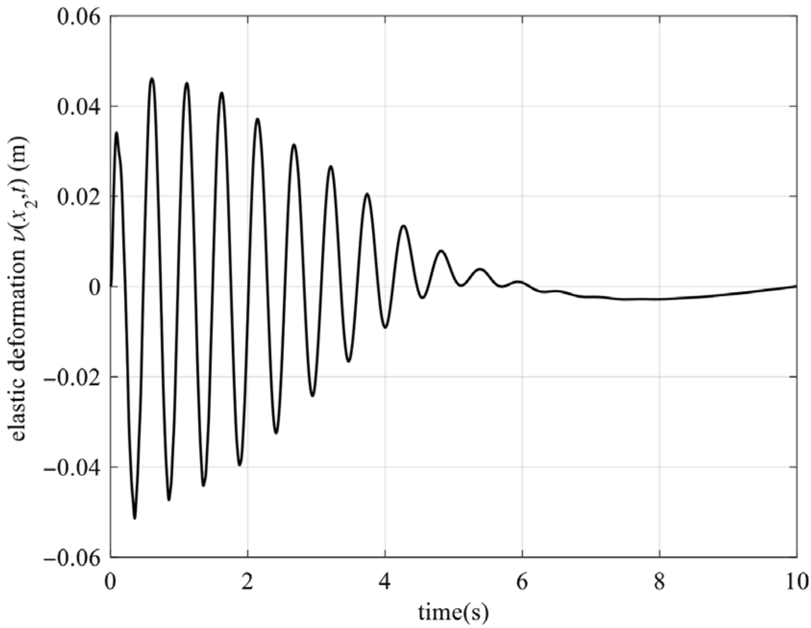

Figure 11. *The flexible link's deformation.*

can accurately track the desired trajectory (the error is only 0.015 rad). The flexible link's deformation is compensated. The vibrations caused by the flexible joints and the flexible link can be suppressed.

The comparison experiments are also taken in simulation 2 to prove the effectiveness of the hybrid control:

Case 1: Turn off the fuzzy controller $\boldsymbol{u}_3$. The simulation results are shown in Figs. 13 and 14. We can find that, when $\boldsymbol{u}_3$ is closed, the system's tracking errors and the flexible-joints angle errors increase, the control precision decreases.

https://doi.org/10.1017/S0263574721000977 Published online by Cambridge University Press

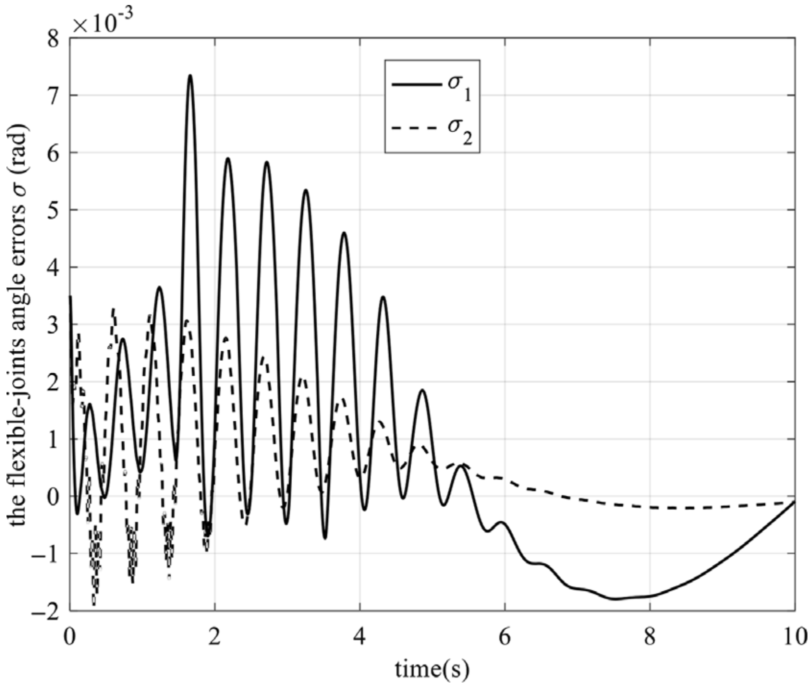

Figure 12. *The flexible-joints angle errors σ.*

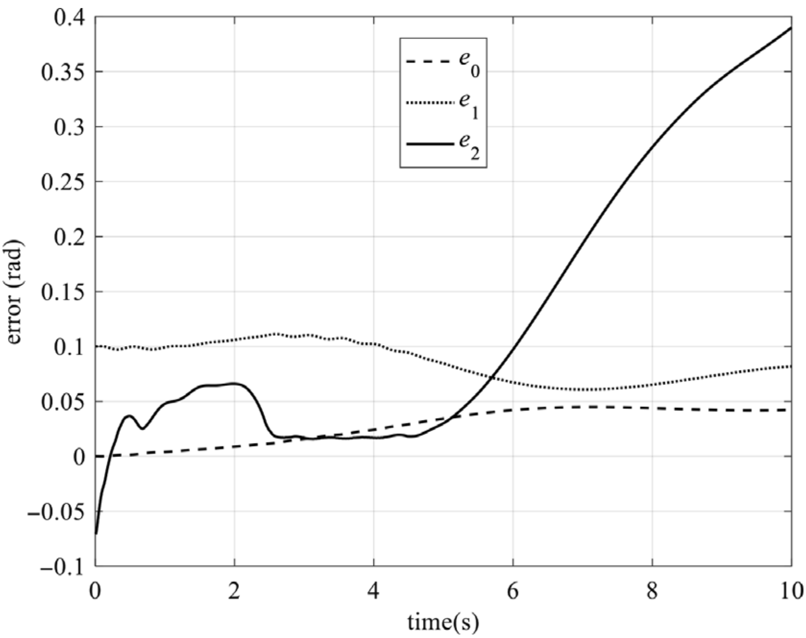

Figure 13. *The space manipulator trajectory tracking errors when $\boldsymbol{u}_3$ is closed.*

https://doi.org/10.1017/S0263574721000977 Published online by Cambridge University Press

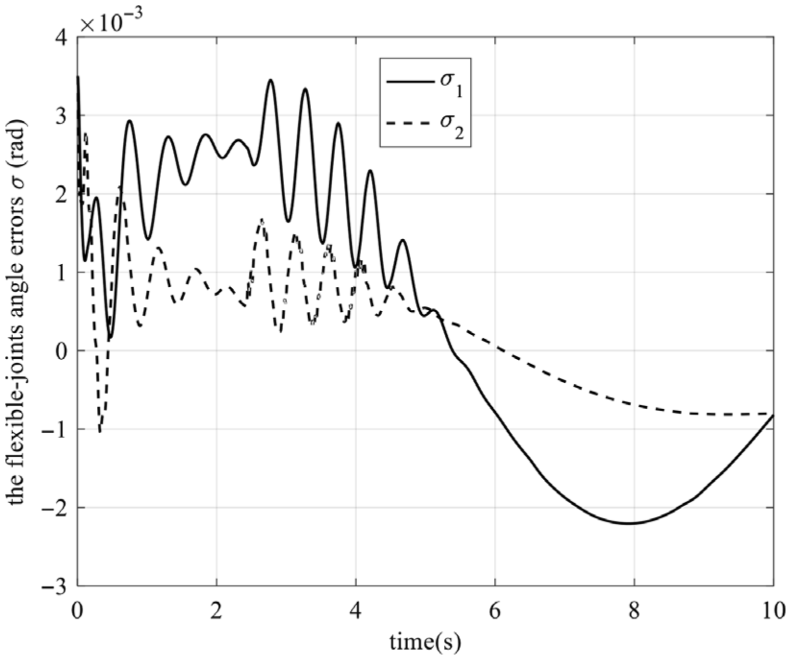

Figure 14. *The flexible-joints angle errors σ when $\boldsymbol{u}_3$ is closed.*

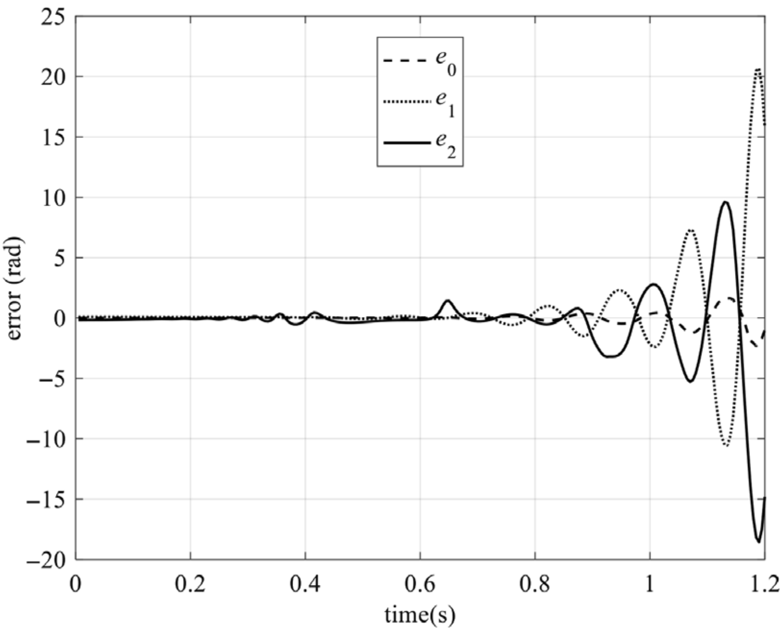

Figure 15. *The space manipulator trajectory tracking errors when $\boldsymbol{\tau}_{\mathrm{f}}$ is closed.*

Case 2: Turn off the fast controller $\boldsymbol{\tau}_{\mathrm{f}}$. The simulation results are shown in Figs. 15–18. We can find that, when $\boldsymbol{\tau}_{\mathrm{f}}$ is closed, the trajectory tracking errors and the flexible-joints angle errors became large in <1.2 s, the flexible-link's vibration cannot be suppressed and its deformation cannot be compensated. That is, the system fails to track. So, the effectiveness of $\boldsymbol{\tau}_{\mathrm{f}}$ is proved.

https://doi.org/10.1017/S0263574721000977 Published online by Cambridge University Press

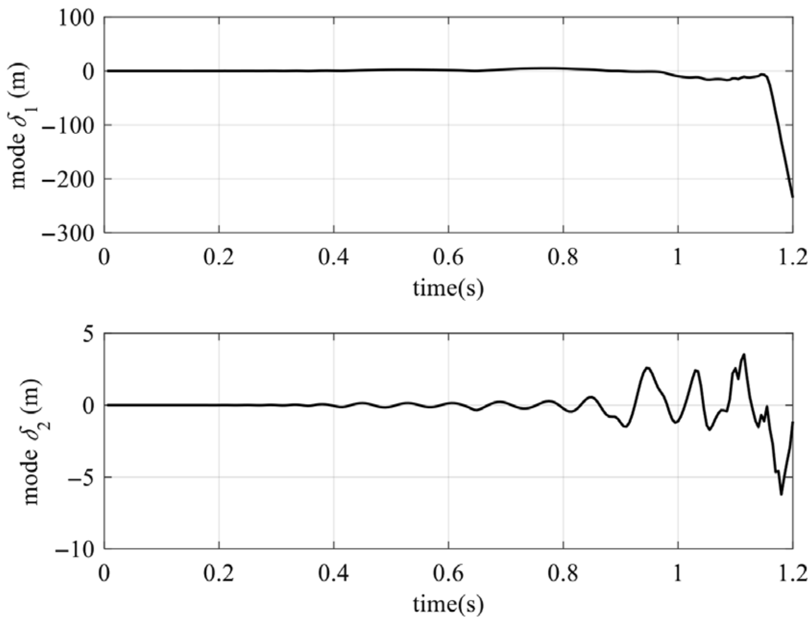

Figure 16. *The flexible link's mode coordinate when $\boldsymbol{\tau}_f$ is closed.*

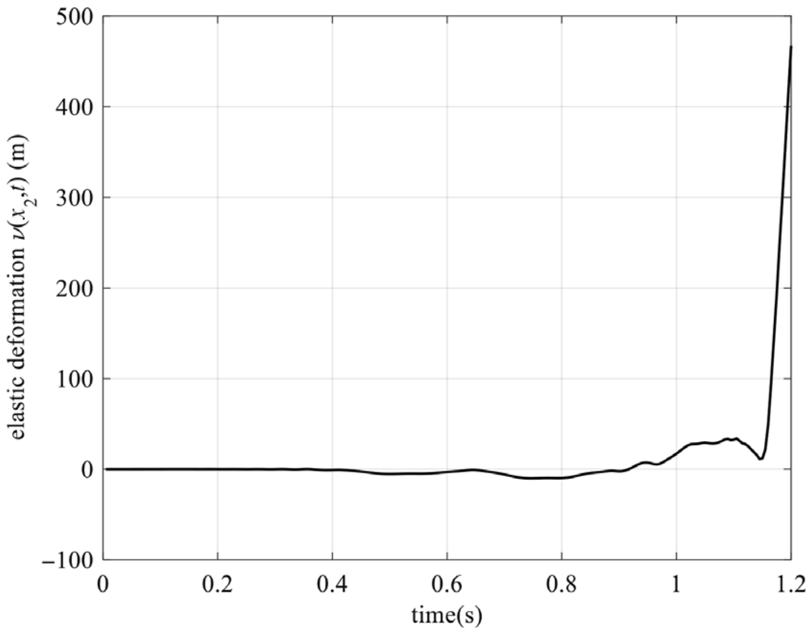

Figure 17. *The flexible link's deformation when $\boldsymbol{\tau}_f$ is closed.*

5. Conclusion

In this paper, the free-floating space manipulator system with flexible-joints, flexible-link, uncertain parameters, and external interference is studied. First, combining the assumed mode method, the system's linear momentum conservation, angular momentum conservation, and Lagrange equation, the system's dynamic equation is established. Considering that this is a rigid-flexible hybrid system, the system dynamics singular perturbation model is established according to the singular perturbation method.

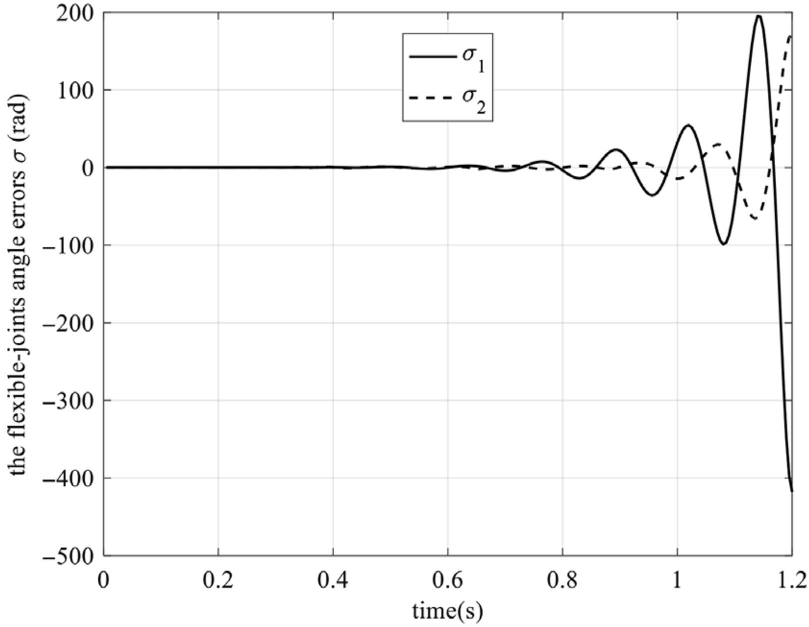

Figure 18. *The flexible-joints angle errors σ when $\boldsymbol{\tau}_f$ is closed.*

Then, a hybrid control is proposed, composed of the slow subsystem's robust fuzzy sliding mode control, the flexible-joints fast subsystem's speed difference feedback control, and the flexible-link fast subsystem's linear-quadratic optimal control. The MATLAB simulations with different desired trajectories and external interference are taken. The simulation results proved that the hybrid control could control the system to track the desired trajectory accurately and suppress the vibration caused by the flexible joints and the flexible link. The controller has the advantages of real-time feedback, self-adaptation, and fewer calculations.

However, we also found that the error's convergence speed is not fast enough, the vibration is evident at the initial stage of the response, and the results did not reach the optimal state. That may be related to the strong coupling and non-linearity of the system and the double flexibility. Improving and optimizing the control performance will be my main task in the future.

Acknowledgments. This research is supported by the National Natural Science Foundation of China (No. 51741502, 11372073, and 11072061).

Conflicts of Interest. The author(s) declare none.

References

[1] L. B. Holcomb and M. D. Montemerlo, "NASA automation and robotics technology program," *IEEE Aerospace Electron. Syst. Mag.* **2**(4), 19–26 (2009).

[2] Y. Fukushima, N. Inaba and M. Oda, "Capture and Berthing Experiment of a Massive Object Using ETS-VII's Space Robot-World's First on-Orbit Satellite Capture Experiment by Space Robot System," American Institute of Aeronautics and Astronautics Astrodynamics Specialist Conference (2000) pp. 634–638.

[3] M. M. Wang, J. J. Luo and U. Walter, "A non-linear model predictive controller with obstacle avoidance for a space robot," Adv. Space Res. **57**(8), 1737–1746 (2016).

[4] M. D. Stefano, R. Balachandran and C. Secchi, "A passivity-based approach for simulating satellite dynamics with robots: Discrete-time integration and time-delay compensation," IEEE Trans. Rob. **36**(1), 189–203 (2020).

[5] M. Oda, "Attitude control experiments of a robot satellite", *J. Spacecraft Rockets* **37**(6), 788–793 (2015).

[6] M. Oda and Y. Fukushima, "Dynamics and control of a robot satellite," *J. Rob. Soc. Jpn* **17**(8), 1067–1071 (2010).

[7] M. M. Wang, J. J. Luo and U. Walter, "Trajectory planning of free-floating space robot using Particle Swarm Optimization (PSO)," *Acta Astronautica* **112**, 77–88 (2015).
[8] F. A. Angel, M. Ou, P. Khanh and U. Steve, "A review of space robotics technologies for on-orbit servicing," *Prog. Aerospace Sci.* **68**, 1–26 (2014).
[9] T. Rybus, K. Seweryn and J. Z. Sasiadek, "Control system for free-floating space manipulator based on nonlinear model predictive control (NMPC)," *J. Intell. Robot Syst.* **85**(3–4), 491–509 (2017).
[10] D. King, "Space Servicing: Past, Present and Future," Proceedings of the 6th International Symposium on Artificial Intelligence and Robotics & Automation in Space (2001).
[11] Y. Q. Zhou, J. J. Luo and M. M. Wang, "Dynamic manipulability analysis of multi-arm space robot," *Robotica* **39**(1), 1–19 (2020).
[12] W. F. Xu, Y. Liu and Y. S. Xu, "The coordinated motion planning of a dual-arm space robot for target capturing," *Robotica* **30**(5), 755–771 (2012).
[13] Y. S. Xu, Y. L. Gu, Y. T. Wu and R. Sclabassi, "Robust control of free-floating space robot systems," *Int. J. Control* **61**(2), 261–277 (1995).
[14] P. M. Pathak, R. P. Kumar, A. Mukherjee and A. Dasgupta, "A scheme for robust trajectory control of space robots," *Simul. Modell. Pract. Theory* **16**(9), 1337–1349 (2008).
[15] Z. Y. Chu, F. C. Sun and J. Cui, "Disturbance observer-based robust control of free-floating space manipulators," *IEEE Syst. J.* **2**(1), 114–119 (2008).
[16] O. Parlaktuna and M. Ozkan, "Adaptive control of free-floating space manipulators using dynamically equivalent manipulator model," *Rob. Auto. Syst.* **46**(3), 185–193 (2004).
[17] S. Abiko and G. Hirzinger, "An Adaptive Control for a Free-Floating Space Robot by Using Inverted Chain Approach," IEEE/RSJ International Conference on Intelligent Robots and Systems (2007) pp. 2236–2241.
[18] S. Abiko and G. Hirzinger, "Adaptive Control for a Torque Controlled Free-Floating Space Robot with Kinematic and Dynamic Model Uncertainty," IEEE/RSJ International Conference on Intelligent Robots and Systems (2009) pp. 2359–2364.
[19] F. C. Liu, L. H. Liang and J. J. Gao, "Fuzzy PID control of space manipulator for both ground alignment and space applications," *Int. J. Autom. Comput.* **11**(4), 353–360 (2014).
[20] J. Cheng and L. Chen, "The fuzzy neural network control scheme with H-infinity tracking characteristic of space robot system with dual-arm after capturing a spin spacecraft," *IEEE-CAA J. Autom. Sinica* **7**(5), 1417–1424 (2020).
[21] Y. S. Guo and C. Li, "Adaptive neural network control for coordinated motion of a dual-arm space robot system with uncertain parameters," *Appl. Math. Mech.* **29**(9), 1131–1140 (2008).
[22] V. Yu. Rutkovskii, V. M. Sukhanov and V. M. Glumov, "Control of multimode manipulative space robot in outer space," *Autom. Remote Control* **71**(11), 2345–2359 (2010).
[23] A. Pisculli, L. Felicetti, P. Gasbarri, G. B. Palmerini and M. Sabatimi, "A reaction-null/Jacobian transpose control strategy with gravity gradient compensation for on-orbit space manipulators," *Aerospace Sci. Technol.* **38**, 30–40 (2014).
[24] Z. Y. Chu, J. Cui and F. C. Sun, "Fuzzy adaptive disturbance-observer-based robust tracking control of electrically driven free-floating space manipulator," *IEEE Syst. J.* **8**(2), 343–352 (2014).
[25] F. H. Zhang, Y. L. Fu, J. D. Qu and S. G. Wang, "Robust adaptive control of a free-floating space robot system in Cartesian space," Int. J. Adv. Rob. Syst. **12**(11), 157 (2015).
[26] S. Kalaycioglu and A. Brown, "Adaptive hybrid force/position control for the Space Station Alpha robotic operations," *Robotica* **13**(6), 549–557 (1995).
[27] B. Siciliano and W. J. Book, "A singular perturbation approach to control of lightweight flexible manipulators," *Int. J. Rob. Res.* **7**(4), 79–90 (1988).
[28] A. Benosman and G. Le Vey, "Control of flexible manipulators: A survey," *Robotica* **22**(05), 533–545 (2004).
[29] P. Zarafshan, S. Ali, A. Moosavian and E. G. Papadopoulos, "Adaptive hybrid suppression control of space free-flying robots with flexible appendages," *Robotica* **34**(7), 1464–1485 (2016).
[30] M. W. Spong, "Adaptive control of flexible joint manipulators: Comments on two papers," *Automatica* **31**(4), 585–590 (1995).
[31] S. Ozgoli and H. D. Taghirad, "A survey on the control of flexible joint robots," *Asian J. Control* **8**(4), 332–344 (2010).
[32] S. K. Dwivedy and P. Eberhard, "Dynamic analysis of flexible manipulators, a literature review," *Mech. Mach. Theory* **41**(7), 749–777 (2006).
[33] T. Komats and V. J. Modi, "Dynamical analysis for task configuration of redundant flexible space manipulator on space platform," IFAC Proc. Vol. 37(6), 363–368 (2004).
[34] H. Wu, F. C. Sun, Z. Q. Sun and L. C. Wu, "Optimal trajectory planning of a flexible dual-arm space robot with vibration reduction," *J. Intell. Rob. Syst.* **40**(2), 147–163 (2004).
[35] L. M. Xie and L. Chen, "Robust and adaptive control of free-floating flexible space manipulator with bounded control torques," *J. Mech. Eng.* **48**(21), 41–46 (2012).
[36] M. Sabatini, P. Gasbarri, R. Monti and G. B. Palmerini, "Vibration control of a flexible space manipulator during on orbit operations," *Acta Astronautica* **73**, 109–121 (2012).
[37] X. Q. Huang, X. T. Tang and L. Chen, "Simulation for trajectory tracking of multi-flexible-link space robot with deadzone," *Int. J. Simul. Modell.* **17**(4), 677–689 (2018).
[38] A. Kumar, P. M. Pathak and N. Sukavanam, "Reduced model based control of two link flexible space robot," *Intell. Control Autom.* **2**(2), 112–120 (2011).
[39] S. Kayastha, J. Katupitiya and G. Pearce, "Control of a Space Robot with Flexible Manipulator Using Generalized Decoupling Technique," 2018 2nd International Conference on Robotics and Automation Sciences(ICRAS) (2018) pp. 1–6.

[40] X. Y. Yu and L. Chen, “Observer-based two-time scale robust control of free-flying flexible-joint space manipulators with external disturbances,” Robotica 35(11), 2201–2217 (2017).
[41] K. Nanos and E. G. Papadopoulos, “On the dynamics and control of flexible joint space manipulators,” *Control Eng. Pract.* **45**, 230–243 (2015).
[42] S. Ulrich, J. Z. Sasiadek and I. Barkana, “Modeling and direct adaptive control of a flexible-joint manipulator,” *J. Guidance Control Dyn.* **35**(1), 25–39 (2012).
[43] S. Ulrich and J. Z. Sasiadek, “Extended Kalman Filtering for Flexible Joint Space Robot Control,” American Control Conference IEEE (2011) pp. 1021–1026.
[44] S. Ulrich, J. Z. Sasiadek and I. Barkana, “Nonlinear Adaptive Output Feedback Control of Flexible-Joint Space Robot Manipulators,” AIAA Guidance, Navigation, and Control Conference (2013) pp. 1–24.
[45] J. Liang, P. Han, L. Chen and Q. K. Yu, “Radial Basis Function Neural Network Adaptive Control of Flexible-Joint Space Robot,” IEEE 2018 Chinese Automation Congress (CAC) (2018) pp. 1569–1574.
[46] P. Dong, Z. Yang, Z. Yue, W. Cheng and E. Wei, “Dynamic modeling and analysis of space manipulator considering the flexible of joint and link,” *Adv. Mater. Res.* **823**, 270–275 (2013).
[47] L. M. Xie and L. Chen, “Nonlinear sliding mode motion control and double elastic vibration active suppression of free-floating flexible-joint and flexible-link space robot,” *China Mech. Eng.* **24**(19), 2657–2663 (2013).
[48] Q. Zhang, X. F. Liu and G. P. Cai, “Dynamics and control of a flexible-link flexible-joint space robot with joint friction,” *Int. J. Aeronaut. Space Sci.* **22**(2), 415–432 (2021).
[49] X. Y. Yu, “Augmented robust control of a free-floating flexible space robot,” *J. Aerospace Eng.* **229**(5), 947–957 (2015).
[50] L. J. Zhang and L. Chen, “ L_2 -gain roust control for flexible joints and flexible link space robot,” *J. Syst. Simul.* **30**(4), 1448–1455 (2018).
[51] G. Feng and M. Palaniswami, “Adaptive control of robot manipulators in task space,” IEEE Trans. Autom. *Control* **38**(1), 100–104 (1993).
[52] M. W. Spong and R. Ortega, “On adaptive inverse dynamics control of rigid robots,” IEEE Trans. Autom. *Control* **35**(1), 92–95 (1990).
[53] S. Dubowsky and E. Papadopoulos, “The kinematics, dynamics, and control of free-flying and free-floating space robotic systems,” IEEE Trans. Rob. Autom. **9**(5), 531–543 (1993).
[54] G. Cai and J. Hong, “Assumed mode method of a rotating flexible beam,” *Acta Mechanica Sinica* **37**(1), 48–56 (2005).
[55] P. V. Kokotovic, “Singular perturbation methods in control,” *Automatica* **25**(6), 953–954 (1989).
[56] A. Bemporad, M. Morari, V. Dua and E. N. Pistikopoulos, “The explicit linear quadratic regulator for constrained systems,” *Automatica* **38**(1), 3–20 (2002).
[57] M. W. Spong, “Modeling and control of elastic joint robots,” *J. Dyn. Syst. Meas. Control* **109**(4), 310–319 (1987).
[58] A. M. Krall, “Asymptotic stability of the Euler-Bernoulli beam with boundary control,” *J. Math. Anal. Appl.* **137**(1), 288–295 (1989).
[59] Z. F. Guo, G. G. Jin, B. Y. Chang and Y. Wang, “Research of dynamic modeling and performance for rigid-flexible manipulators,” *J. Tianjin Poltechnic Univ.* **32**(1), 70–74, (2013).
[60] Y. G. Lv, Y. D. Wei and Z. C. Chen, “Active control on coupled bending-torsion vibration of two-link space flexible component,” *J. Zhejiang Univ. (Eng. Sci.)* **41**(5), 715–719 (2007).
[61] M. W. Spong, “Adaptive control of flexible joint manipulators,” *Syst. Control Lett.* **13**(1), 15–21 (1989).
[62] J. E. Slotin and W. P. Li, “On the adaptive control of robot manipulators,” *J. Rob. Res.* **6**(3), 49–59 (1987).
[63] S. Koskie, C. Couomarbatch and Z. Gajic, “Exact slow-fast decomposition of the singularly perturbed matrix differential Riccati equation,” *Appl. Math. Comput.* **216**(5), 1401–1411 (2010).

Appendix: $\boldsymbol{M}(q, \delta)$ and $\boldsymbol{H}(q, \dot{q}, \delta, \dot{\delta})$ in Dynamic Eq. (10)

$$\begin{aligned}\boldsymbol{M}(1,1) = {} & 2\Gamma_1 + 2\Gamma_2 + 2\Gamma_3 + 2\Gamma_4\delta_1^2 + 2\Gamma_5\delta_2^2 + 2\Gamma_6 \cos(q_1) + 2\Gamma_7 \cos(q_1+q_2) - 2\Gamma_8\delta_1 \sin(q_1+q_2) \\ & - 2\Gamma_9\delta_2 \sin(q_1+q_2) + 2\Gamma_{10}\cos(q_2) - 2\Gamma_{11}\delta_1 \sin(q_2) - 2\Gamma_{12}\delta_2 \sin(q_2) + 2\Gamma_{13}\delta_1\delta_2\end{aligned}$$

$$\begin{aligned}\boldsymbol{M}(1,2) = {} & 2\Gamma_2 + 2\Gamma_3 + 2\Gamma_4\delta_1^2 + 2\Gamma_5\delta_2^2 + \Gamma_6 \cos(q_1) + \Gamma_7 \cos(q_1+q_2) - \Gamma_8\delta_1 \sin(q_1+q_2) \\ & - \Gamma_9\delta_2 \sin(q_1+q_2) + 2\Gamma_{10}\cos(q_2) - 2\Gamma_{11}\delta_1 \sin(q_2) - 2\Gamma_{12}\delta_2 \sin(q_2) + 2\Gamma_{13}\delta_1\delta_2\end{aligned}$$

$$\begin{aligned}\boldsymbol{M}(1,3) = {} & 2\Gamma_3 + 2\Gamma_4\delta_1^2 + 2\Gamma_5\delta_2^2 + \Gamma_7 \cos(q_1+q_2) - \Gamma_8\delta_1 \sin(q_1+q_2) - \Gamma_9\delta_2 \sin(q_1+q_2) \\ & + \Gamma_{10}\cos(q_2) - \Gamma_{11}\delta_1 \sin(q_2) - \Gamma_{12}\delta_2 \sin(q_2) + 2\Gamma_{13}\delta_1\delta_2\end{aligned}$$

$$\boldsymbol{M}(1,4) = \Gamma_8 \cos(q_1+q_2) + \Gamma_{11}\cos(q_2) + \Gamma_{14}$$

$$\boldsymbol{M}(1,5) = \Gamma_9 \cos(q_1+q_2) + \Gamma_{12}\cos(q_2) + \Gamma_{15}$$

https://doi.org/10.1017/S0263574721000977 Published online by Cambridge University Press

$$\boldsymbol{M}(2,1)=\boldsymbol{M}(1,2)$$

$$\boldsymbol{M}(2,2)=2\Gamma_2+2\Gamma_3+2\Gamma_4\delta_1^2+2\Gamma_5\delta_2^2+2\Gamma_{10}\cos(q_2)-2\Gamma_{11}\delta_1\sin(q_2)-2\Gamma_{12}\delta_2\sin(q_2)+2\Gamma_{13}\delta_1\delta_2$$

$$\boldsymbol{M}(2,3)=2\Gamma_3+2\Gamma_4\delta_1^2+2\Gamma_5\delta_2^2+\Gamma_{10}\cos(q_2)-\Gamma_{11}\delta_1\sin(q_2)-\Gamma_{12}\delta_2\sin(q_2)+\Gamma_{13}\delta_1\delta_2$$

$$\boldsymbol{M}(2,4)=\Gamma_{11}\cos(q_2)+\Gamma_{14}$$

$$\boldsymbol{M}(2,5)=\Gamma_{12}\cos(q_2)+\Gamma_{15}$$

$$\boldsymbol{M}(3,1)=\boldsymbol{M}(1,3)$$

$$\boldsymbol{M}(3,2)=\boldsymbol{M}(2,3)$$

$$\boldsymbol{M}(3,3)=2\Gamma_3+2\Gamma_4\delta_1^2+2\Gamma_5\delta_2^2+2\Gamma_{13}\delta_1\delta_2$$

$$\boldsymbol{M}(3,4)=\Gamma_{14}$$

$$\boldsymbol{M}(3,5)=\Gamma_{15}$$

$$\boldsymbol{M}(4,1)=\boldsymbol{M}(1,4),\boldsymbol{M}(4,2)=\boldsymbol{M}(2,4),\boldsymbol{M}(4,3)=\boldsymbol{M}(3,4),\boldsymbol{M}(4,4)=2\Gamma_4,\boldsymbol{M}(4,5)=\Gamma_{13}$$

$$\boldsymbol{M}(5,1)=\boldsymbol{M}(1,5),\ \boldsymbol{M}(5,2)=\boldsymbol{M}(2,5),\ \boldsymbol{M}(5,3)=\boldsymbol{M}(3,5),\ \boldsymbol{M}(5,4)=\boldsymbol{M}(4,5),\ \boldsymbol{M}(5,5)=2\Gamma_5$$

$$\begin{aligned}\boldsymbol{H}(1,1)=&\,2\Gamma_4\delta_1\dot{\delta}_1+2\Gamma_5\delta_2\dot{\delta}_2-\Gamma_6\dot{q}_1\sin(q_1)-\Gamma_7(\dot{q}_1+\dot{q}_2)\sin(q_1+q_2)\\&-\Gamma_8[\dot{\delta}_1\sin(q_1+q_2)+\delta_1(\dot{q}_1+\dot{q}_2)\cos(q_1+q_2)]-\Gamma_9[\dot{\delta}_2\sin(q_1+q_2)\\&+\delta_2(\dot{q}_1+\dot{q}_2)\cos(q_1+q_2)]-\Gamma_{10}\dot{q}_2\sin(q_2)-\Gamma_{11}[\dot{\delta}_1\sin(q_2)+\delta_1\dot{q}_2\cos(q_2)]\\&-\Gamma_{12}[\dot{\delta}_2\sin(q_2)+\delta_2\dot{q}_2\cos(q_2)]+\Gamma_{13}(\dot{\delta}_1\delta_2+\delta_1\dot{\delta}_2)\end{aligned}$$

$$\begin{aligned}\boldsymbol{H}(1,2)=&\,2\Gamma_4\delta_1\dot{\delta}_1+2\Gamma_5\delta_2\dot{\delta}_2-\Gamma_6(\dot{q}_1+\dot{q}_2)\sin(q_1)-\Gamma_7(\dot{q}_0+\dot{q}_1+\dot{q}_2)\sin(q_1+q_2)\\&-\Gamma_8[\dot{\delta}_1\sin(q_1+q_2)+\delta_1(\dot{q}_0+\dot{q}_1+\dot{q}_2)\cos(q_1+q_2)]-\Gamma_9[\dot{\delta}_2\sin(q_1+q_2)\\&+\delta_2(\dot{q}_0+\dot{q}_1+\dot{q}_2)\cos(q_1+q_2)]-\Gamma_{10}\dot{q}_2\sin(q_2)-\Gamma_{11}[\dot{\delta}_1\sin(q_2)+\delta_1\dot{q}_2\cos(q_2)]\\&-\Gamma_{12}[\dot{\delta}_2\sin(q_2)+\delta_2\dot{q}_2\cos(q_2)]+\Gamma_{13}(\dot{\delta}_1\delta_2+\delta_1\dot{\delta}_2)\end{aligned}$$

$$\begin{aligned}\boldsymbol{H}(1,3)=&\,2\Gamma_4\delta_1\dot{\delta}_1+2\Gamma_5\delta_2\dot{\delta}_2-\Gamma_7(\dot{q}_0+\dot{q}_1+\dot{q}_2)\sin(q_1+q_2)-\Gamma_8[\dot{\delta}_1\sin(q_1+q_2)\\&+\delta_1(\dot{q}_0+\dot{q}_1+\dot{q}_2)\cos(q_1+q_2)]-\Gamma_9[\dot{\delta}_2\sin(q_1+q_2)+\delta_2(\dot{q}_0+\dot{q}_1+\dot{q}_2)\cos(q_1+q_2)]\\&-\Gamma_{10}(\dot{q}_0+\dot{q}_1+\dot{q}_2)\sin(q_2)-\Gamma_{11}[\dot{\delta}_1\sin(q_2)+\delta_1(\dot{q}_0+\dot{q}_1+\dot{q}_2)\cos(q_2)]\\&-\Gamma_{12}[\dot{\delta}_2\sin(q_2)+\delta_2(\dot{q}_0+\dot{q}_1+\dot{q}_2)\cos(q_2)]+\Gamma_{13}(\dot{\delta}_1\delta_2+\delta_1\dot{\delta}_2)\end{aligned}$$

$$\begin{aligned}\boldsymbol{H}(1,4)=&\,2\Gamma_4\delta_1(\dot{q}_0+\dot{q}_1+\dot{q}_2)-\Gamma_8(\dot{q}_0+\dot{q}_1+\dot{q}_2)\sin(q_1+q_2)-\Gamma_{11}(\dot{q}_0+\dot{q}_1+\dot{q}_2)\sin(q_2)\\&+\Gamma_{13}\delta_2(\dot{q}_0+\dot{q}_1+\dot{q}_2)\end{aligned}$$

$$\begin{aligned}\boldsymbol{H}(1,5)=&\,2\Gamma_5\delta_2(\dot{q}_0+\dot{q}_1+\dot{q}_2)-\Gamma_9(\dot{q}_0+\dot{q}_1+\dot{q}_2)\sin(q_1+q_2)-\Gamma_{12}(\dot{q}_0+\dot{q}_1+\dot{q}_2)\sin(q_2)\\&+\Gamma_{13}\delta_1(\dot{q}_0+\dot{q}_1+\dot{q}_2)\end{aligned}$$

$$\begin{aligned}\boldsymbol{H}(2,1)=&\,2\Gamma_4\delta_1\dot{\delta}_1+2\Gamma_5\delta_2\dot{\delta}_2+\Gamma_6\dot{q}_0\sin(q_1)+\Gamma_7\dot{q}_0\sin(q_1+q_2)+\Gamma_8\delta_1\dot{q}_0\cos(q_1+q_2)\\&+\Gamma_9\delta_2\dot{q}_0\cos(q_1+q_2)-\Gamma_{10}\dot{q}_2\sin(q_2)-\Gamma_{11}[\dot{\delta}_1\sin(q_2)+\delta_1\dot{q}_2\cos(q_2)]\\&-\Gamma_{12}[\dot{\delta}_2\sin(q_2)+\delta_2\dot{q}_2\cos(q_2)]+\Gamma_{13}(\dot{\delta}_1\delta_2+\delta_1\dot{\delta}_2)\end{aligned}$$

https://doi.org/10.1017/S0263574721000977 Published online by Cambridge University Press

$$\boldsymbol{H}(2,2)=2\Gamma_4\delta_1\dot{\delta}_1+2\Gamma_5\delta_2\dot{\delta}_2-\Gamma_{10}\dot{q}_2\sin(q_2)-\Gamma_{11}[\dot{\delta}_1\sin(q_2)+\delta_1\dot{q}_2\cos(q_2)]-\Gamma_{12}[\dot{\delta}_2\sin(q_2)+\delta_2\dot{q}_2\cos(q_2)]+\Gamma_{13}(\dot{\delta}_1\delta_2+\delta_1\dot{\delta}_2)$$

$$\boldsymbol{H}(2,3)=2\Gamma_4\delta_1\dot{\delta}_1+2\Gamma_5\delta_2\dot{\delta}_2-\Gamma_{10}(\dot{q}_0+\dot{q}_1+\dot{q}_2)\sin(q_2)-\Gamma_{11}[\dot{\delta}_1\sin(q_2)+\delta_1(\dot{q}_0+\dot{q}_1+\dot{q}_2)\cos(q_2)]-\Gamma_{12}[\dot{\delta}_2\sin(q_2)+\delta_2(\dot{q}_0+\dot{q}_1+\dot{q}_2)\cos(q_2)]+\Gamma_{13}(\dot{\delta}_1\delta_2+\delta_1\dot{\delta}_2)$$

$$\boldsymbol{H}(2,4)=2\Gamma_4\delta_1(\dot{q}_0+\dot{q}_1+\dot{q}_2)-\Gamma_{11}(\dot{q}_0+\dot{q}_1+\dot{q}_2)\sin(q_2)+\Gamma_{13}\delta_2(\dot{q}_0+\dot{q}_1+\dot{q}_2)$$

$$\boldsymbol{H}(2,5)=2\Gamma_5\delta_2(\dot{q}_0+\dot{q}_1+\dot{q}_2)-\Gamma_{12}(\dot{q}_0+\dot{q}_1+\dot{q}_2)\sin(q_2)+\Gamma_{13}\delta_1(\dot{q}_0+\dot{q}_1+\dot{q}_2)$$

$$\boldsymbol{H}(3,1)=2\Gamma_4\delta_1\dot{\delta}_1+2\Gamma_5\delta_2\dot{\delta}_2+\Gamma_7\dot{q}_0\sin(q_1+q_2)+\Gamma_8\delta_1\dot{q}_0\cos(q_1+q_2)+\Gamma_9\delta_2\dot{q}_0\cos(q_1+q_2)+\Gamma_{10}(\dot{q}_0+\dot{q}_1)\sin(q_2)+\Gamma_{11}\delta_1(\dot{q}_0+\dot{q}_1)\cos(q_2)+\Gamma_{12}\delta_2(\dot{q}_0+\dot{q}_1)\cos(q_2)+\Gamma_{13}(\dot{\delta}_1\delta_2+\delta_1\dot{\delta}_2)$$

$$\boldsymbol{H}(3,2)=2\Gamma_4\delta_1\dot{\delta}_1+2\Gamma_5\delta_2\dot{\delta}_2+\Gamma_{10}(\dot{q}_0+\dot{q}_1)\sin(q_2)+\Gamma_{11}\delta_1(\dot{q}_0+\dot{q}_1)\cos(q_2)+\Gamma_{12}\delta_2(\dot{q}_0+\dot{q}_1)\cos(q_2)+\Gamma_{13}(\dot{\delta}_1\delta_2+\delta_1\dot{\delta}_2)$$

$$\boldsymbol{H}(3,3)=2\Gamma_4\delta_1\dot{\delta}_1+2\Gamma_5\delta_2\dot{\delta}_2+\Gamma_{13}(\dot{\delta}_1\delta_2+\delta_1\dot{\delta}_2)$$

$$\boldsymbol{H}(3,4)=2\Gamma_4\delta_1(\dot{q}_0+\dot{q}_1+\dot{q}_2)+\Gamma_{13}\delta_2(\dot{q}_0+\dot{q}_1+\dot{q}_2)$$

$$\boldsymbol{H}(3,5)=2\Gamma_5\delta_2(\dot{q}_0+\dot{q}_1+\dot{q}_2)+\Gamma_{13}\delta_1(\dot{q}_0+\dot{q}_1+\dot{q}_2)$$

$$\boldsymbol{H}(4,1)=-2\Gamma_4\delta_1(\dot{q}_0+\dot{q}_1+\dot{q}_2)+\Gamma_8\dot{q}_0\sin(q_1+q_2)+\Gamma_{11}(\dot{q}_0+\dot{q}_1)\sin(q_2)-\Gamma_{13}\delta_2(\dot{q}_0+\dot{q}_1+\dot{q}_2)$$

$$\boldsymbol{H}(4,2)=-2\Gamma_4\delta_1(\dot{q}_0+\dot{q}_1+\dot{q}_2)+\Gamma_{11}(\dot{q}_0+\dot{q}_1)\sin(q_2)-\Gamma_{13}\delta_2(\dot{q}_0+\dot{q}_1+\dot{q}_2)$$

$$\boldsymbol{H}(4,3)=-2\Gamma_4\delta_1(\dot{q}_0+\dot{q}_1+\dot{q}_2)-\Gamma_{13}\delta_2(\dot{q}_0+\dot{q}_1+\dot{q}_2)$$

$$\boldsymbol{H}(4,4)=0$$

$$\boldsymbol{H}(4,5)=0$$

$$\boldsymbol{H}(5,1)=-2\Gamma_5\delta_2(\dot{q}_0+\dot{q}_1+\dot{q}_2)+\Gamma_9\dot{q}_0\sin(q_1+q_2)+\Gamma_{12}(\dot{q}_0+\dot{q}_1)\sin(q_2)-\Gamma_{13}\delta_1(\dot{q}_0+\dot{q}_1+\dot{q}_2)$$

$$\boldsymbol{H}(5,2)=-2\Gamma_5\delta_2(\dot{q}_0+\dot{q}_1+\dot{q}_2)+\Gamma_{12}(\dot{q}_0+\dot{q}_1)\sin(q_2)-\Gamma_{13}\delta_1(\dot{q}_0+\dot{q}_1+\dot{q}_2)$$

$$\boldsymbol{H}(5,3)=-2\Gamma_5\delta_2(\dot{q}_0+\dot{q}_1+\dot{q}_2)-\Gamma_{13}\delta_1(\dot{q}_0+\dot{q}_1+\dot{q}_2)$$

$$\boldsymbol{H}(5,4)=0$$

$$\boldsymbol{H}(5,5)=0$$

where

$$\Gamma_1=\frac{1}{2}\left(m_0R_{00}^2+m_1R_{10}^2+m_2R_{20}^2+J_0\right),\ \Gamma_2=\frac{1}{2}\left(m_0R_{01}^2+m_1R_{11}^2+m_2R_{21}^2+J_1\right),$$

$$\Gamma_3=\frac{1}{2}\left(m_0R_{02}^2+m_1R_{12}^2+\rho\int_0^{l_2}R_{22}^2\mathrm{d}\boldsymbol{x}_2\right),\ \Gamma_4=\frac{1}{2}\left(m_0R_{03}^2+m_1R_{13}^2+\rho\int_0^{l_2}R_{23}^2\mathrm{d}\boldsymbol{x}_2\right)$$

$$\Gamma_5=\frac{1}{2}\left(m_0R_{04}^2+m_1R_{14}^2+\rho\int_0^{l_2}R_{24}^2\mathrm{d}\boldsymbol{x}_2\right),\ \Gamma_6=m_0R_{00}R_{01}+m_1R_{10}R_{11}+m_2R_{20}R_{21},$$

$$\Gamma_7 = m_0R_{00}R_{02} + m_1R_{10}R_{12} + \rho \int_0^{l_2} R_{20}R_{22}\mathrm{d}\boldsymbol{x}_2,\ \Gamma_8 = m_0R_{00}R_{03} + m_1R_{10}R_{13} + \rho \int_0^{l_2} R_{20}R_{23}\mathrm{d}\boldsymbol{x}_2,$$

$$\Gamma_9 = m_0R_{00}R_{04} + m_1R_{10}R_{14} + \rho \int_0^{l_2} R_{20}R_{24}\mathrm{d}\boldsymbol{x}_2,\ \Gamma_{10} = m_0R_{01}R_{02} + m_1R_{11}R_{12} + \rho \int_0^{l_2} R_{21}R_{22}\mathrm{d}\boldsymbol{x}_2,$$

$$\Gamma_{11} = m_0R_{01}R_{03} + m_1R_{11}R_{13} + \rho \int_0^{l_2} R_{21}R_{23}\mathrm{d}\boldsymbol{x}_2,\ \Gamma_{12} = m_0R_{01}R_{04} + m_1R_{11}R_{14} + \rho \int_0^{l_2} R_{21}R_{24}\mathrm{d}\boldsymbol{x}_2$$

$$\Gamma_{13} = m_0R_{03}R_{04} + m_1R_{13}R_{14} + \rho \int_0^{l_2} R_{23}R_{24}\mathrm{d}\boldsymbol{x}_2,\quad \Gamma_{14} = m_0R_{02}R_{03} + m_1R_{12}R_{13} + \rho \int_0^{l_2} R_{22}R_{23}\mathrm{d}\boldsymbol{x}_2$$

$$\Gamma_{15} = m_0R_{02}R_{04} + m_1R_{12}R_{14} + \rho \int_0^{l_2} R_{22}R_{24}\mathrm{d}\boldsymbol{x}_2.$$

Cite this article: L. Xie, X. Yu and L. Chen (2022). “Robust fuzzy sliding mode control and vibration suppression of free-floating flexible-link and flexible-joints space manipulator with external interference and uncertain parameter”, Robotica **40**, 997–1019. https://doi.org/10.1017/S0263574721000977